

UNIVERSIDAD AUTÓNOMA DE NUEVO LEÓN
FACULTAD DE INGENIERÍA MECÁNICA Y ELÉCTRICA



**THERMOMECHANICAL PERFORMANCE OF FR-4 LAMINATES IN
THE MANUFACTURING PROCESS OF PRINTED CIRCUIT
BOARDS**

POR

CARLOS ALFONSO RODRÍGUEZ VÁZQUEZ

**COMO REQUISITO PARA OBTENER EL GRADO DE
DOCTOR EN INGENIERÍA DE MATERIALES**

AGOSTO, 2016

**UNIVERSIDAD AUTÓNOMA DE NUEVO LEÓN
FACULTAD DE INGENIERÍA MECÁNICA Y ELÉCTRICA
SUBDIRECCIÓN DE ESTUDIOS DE POSGRADO**



**THERMOMECHANICAL PERFORMANCE OF FR-4 LAMINATES IN THE
MANUFACTURING PROCESS OF PRINTED CIRCUIT BOARDS**

POR

CARLOS ALFONSO RODRÍGUEZ VÁZQUEZ

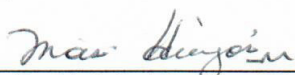
**COMO REQUISITO PARA OBTENER EL GRADO DE
DOCTOR EN INGENIERÍA DE MATERIALES**

AGOSTO, 2016

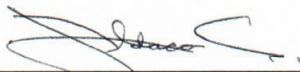
UNIVERSIDAD AUTONOMA DE NUEVO LEON
FACULTAD DE INGENIERIA MECANICA Y ELECTRICA
SUBDIRECCIÓN DE ESTUDIOS DE POSGRADO

Los miembros del Comité de Tesis recomendamos que la Tesis "Thermomechanical Performance of FR-4 Laminates in the Manufacturing Process of Printed Circuit Boards" realizada por el alumno M.C Carlos Alfonso Rodríguez Vázquez, con número de matrícula 1335333, sea aceptada para su defensa como opción al grado de Doctor en Ingeniería de Materiales.

El Comité de Tesis



Dr. Moisés Hinojosa Rivera
Asesor

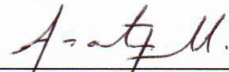


Dr. Jorge Adrián Aldaco Castañeda
Revisor



Dr. Javier Morales Castillo
Revisor

Dr. Carlos Gabriel Morillo Silvera
Revisor



Dra. Ana María Arato Tovar
Revisor

Vo. Bo.

Dr. Simón Martínez Martínez
Subdirector de Estudios de Posgrado

San Nicolás de los Garza, Nuevo León, Agosto 2016

Acknowledgment

This work is dedicated primarily to God and my family who has been at all times to support me to meet each of the goals that, my father Alfonso Rodriguez and my mother Patricia Vázquez they push me to reach my personnel targets being aware of everything that needed.

I appreciate the support of Dr. Moisés Hinojosa for being an excellent advisor, their support was very important for the research work, his collaboration is reflected in the objectives and expectations reached, I appreciate his support for conferences and congress participation.

I appreciate to Dr. Javier Morales, Dr. Jorge Aldaco and Dr. Roberto Cabriaes really for helping during the project meetings we had, making an excellent analysis for knowledge contribution.

I thank Dr. Carlos Morillo and his team at the University of Maryland for enable me and help me to realize experimentation during my stay at CALCE, I learned everything necessary for PCB's characterization and the state of the art.

The National Council of Science and Technology (CONACYT) for providing economic support during these 3 years.

Thanks to Yazaki, especially for Ing. Luis Montes de Oca, EI (Electronic Instruments) manager and Ing. Víctor Salinas Fox who was an important member during the project, Ing. Karla Peña my supervisor at Yazaki for their collaboration to carry out this research, also the staff involved in PCB assembly process at YIM (Yazaki Instruments Monterrey).

Contents

| | |
|--|-----------|
| Acknowledgment | i |
| Abstract | x |
| 1 Introduction | 1 |
| 1.1 What is a Printed Circuit Board? | 1 |
| 1.1.1 Base Materials for Printed Circuit Board | 2 |
| 1.2 Assembly Process of Printed Circuit Board | 3 |
| 2 Literature Overview | 4 |
| 2.1 PCB's Base Materials | 4 |
| 2.1.1 Resins Systems | 5 |
| 2.1.2 Reinforcements | 6 |
| 2.1.3 Conductive Material | 8 |
| 2.2 PCB Fabrication | 10 |
| 2.3 Reflow Process | 11 |
| 2.4 Thermal Properties of PCB Materials | 15 |
| 2.4.1 Glass Transition Temperature | 15 |
| 2.4.2 Decomposition Temperature | 16 |
| 2.4.3 Coefficient of Thermal Expansion | 17 |
| 2.4.4 Time to delamination | 19 |
| 2.4.5 Water Absorption | 21 |
| 2.5 "Bow" and "Twist" | 21 |
| 3 State of the Art | 26 |
| 3.1 Material Properties | 26 |
| 3.2 Reflow Oven Process | 27 |
| 3.3 Warpage | 28 |
| 3.4 Summary | 28 |

| | | |
|----------|--|-----------|
| 4 | Motivation, General Objective, Specific Objectives and Hypothesis | 30 |
| 4.1 | Motivation | 30 |
| 4.2 | General Objective | 31 |
| 4.3 | Specific Objectives | 31 |
| 4.4 | Hypothesis | 32 |
| 5 | Experimental Methodology | 33 |
| 5.1 | Material Characterization | 34 |
| 5.1.1 | PCB configuration | 34 |
| 5.1.2 | Thermal Properties | 34 |
| 5.2 | Reflow Oven | 40 |
| 5.2.1 | Temperature Profiles | 40 |
| 6 | Results and Discussion | 42 |
| 6.1 | Glass Transition Temperature (T _g) | 42 |
| 6.2 | Decomposition Temperature (T _d) | 46 |
| 6.3 | Coefficient of Thermal Expansion | 48 |
| 6.3.1 | Coefficient of Thermal Expansion in the “x” axis | 48 |
| 6.3.2 | Coefficient of Thermal Expansion in the “y” axis | 50 |
| 6.3.3 | Coefficient of Thermal Expansion in the “z” axis | 53 |
| 6.4 | Time to Delamination | 56 |
| 6.5 | Water Absorption | 58 |
| 6.6 | Bow and Twist Measurement | 58 |
| 6.6.1 | PCB “bow” after first reflow | 58 |
| 6.6.2 | PCB “bow” after second reflow | 59 |
| 6.6.3 | PCB “twist” after first reflow | 60 |
| 6.6.4 | PCB “twist” after second reflow | 61 |
| 6.7 | Temperature Profile | 63 |
| 6.8 | Summary of Results | 64 |
| 7 | Conclusions and Contributions | 68 |
| 7.1 | Conclusions | 68 |
| 7.2 | Contributions | 70 |
| A | Heat Transfer for Base Materials | 71 |
| B | PCB’s dimensions | 72 |

| | | |
|----------|---|-----------|
| C | Bow Results | 73 |
| C.1 | Bow results after first reflow | 73 |
| C.2 | Bow results after second reflow | 73 |
| D | Twist Results | 75 |
| D.1 | Twist results after first reflow | 75 |
| D.2 | Twist results after second reflow | 75 |
| | Bibliography | 77 |

List of Figures

| | | |
|------|--|----|
| 1.1 | Sierra GMC indicators panel | 1 |
| 1.2 | Printed Circuit Board | 1 |
| 1.3 | PCB configuration | 2 |
| 1.4 | PCB's manufacturing process diagram | 3 |
| 2.1 | Difunctional epoxy resin reaction | 5 |
| 2.2 | Brominated difunctional epoxy resin reaction | 5 |
| 2.3 | Tetrafunctional epoxy resin | 6 |
| 2.4 | Multifunctional fenol novolac epoxy resin | 6 |
| 2.5 | Glass fiber styles | 7 |
| 2.6 | "Treating" fiberglass cloth with resin | 10 |
| 2.7 | Laminate pressing | 11 |
| 2.8 | Reflow oven | 11 |
| 2.9 | Reflow oven stages | 12 |
| 2.10 | Sn-Ag-Cu Solder paste phase diagram [11] | 13 |
| 2.11 | Sn-Pb Solder paste phase diagram | 13 |
| 2.12 | Cooling area | 14 |
| 2.13 | PCB's Electronic components failure due to PCB "warpage" | 14 |
| 2.14 | Capacitor failure due to PCB "warpage" | 15 |
| 2.15 | Schematic representation to obtain Tg [19] | 16 |
| 2.16 | Decomposition temperature chart for different FR-4 types | 17 |
| 2.17 | Representation to obtain coefficient of thermal expansion | 18 |
| 2.18 | CTE axes | 19 |
| 2.19 | Representation to obtain time to delamination | 20 |
| 2.20 | "Bow" | 22 |
| 2.21 | "Twist" | 22 |
| 2.22 | "bow" y "twist" areas identification | 23 |
| 2.23 | PCB schematic representation of thickness, diagonals and lengths | 24 |

| | | |
|------|--|----|
| 2.24 | PCB schematic representation to obtain % of bow | 24 |
| 2.25 | Schematic representation to obtain % of twist | 25 |
| 5.1 | Experimental procedure | 33 |
| 5.2 | PCB cross sectional view showing PCB ayers configuration | 34 |
| 5.3 | Specimens at different areas of PCB | 35 |
| 5.4 | Preheating oven | 36 |
| 5.5 | DSC Netzch pegasus | 37 |
| 5.6 | Specimens to obtain glass transition temperature | 37 |
| 5.7 | Dynamic Mechanical Analysis (DMA) | 38 |
| 5.8 | Specimens to obtain decomposition temperature | 38 |
| 5.9 | TMA (Thermo Mechanical Analyzer) | 39 |
| 5.10 | Specimens to obtain coefficient of thermal expansion | 39 |
| 5.11 | Specimens water absorption performed | 40 |
| 5.12 | Device to obtain height of the PCB's | 40 |
| 5.13 | PCB to measure oven temperatures | 41 |
| 5.14 | Standard PCB reflow process profile | 41 |
| 6.1 | Glass transition temperature chart top area | 43 |
| 6.2 | Glass transition temperature chart middle area | 43 |
| 6.3 | Glass transition temperature chart bottom area | 44 |
| 6.4 | Decomposition temperature chart | 46 |
| 6.5 | Specimen 1 decomposition temperature chart | 47 |
| 6.6 | Specimen 2 decomposition temperature chart | 47 |
| 6.7 | Coefficient of thermal expansion "x" axis at top area | 48 |
| 6.8 | Coefficient of thermal expansion "x" axis at middle area | 49 |
| 6.9 | Coefficient of thermal expansion "x" axis at bottom area | 49 |
| 6.10 | Coefficient of thermal expansion "y" axis at top area | 51 |
| 6.11 | Coefficient of thermal expansion "y" axis at middle area | 51 |
| 6.12 | Coefficient of thermal expansion "y" axis at bottom area | 52 |
| 6.13 | Coefficient of thermal expansion "z" axis at top area | 53 |
| 6.14 | Coefficient of thermal expansion "z" axis at middle area | 53 |
| 6.15 | Coefficient of thermal expansion "z" axis at bottom area | 54 |
| 6.16 | Time to delamination results at the top | 56 |
| 6.17 | Time to delamination results at the middle | 57 |
| 6.18 | Time to delamination results at the bottom | 57 |
| 6.19 | PCB "bow" results after first reflow | 59 |

| | | |
|------|---|----|
| 6.20 | PCB “bow” results after second reflow | 60 |
| 6.21 | PCB “twist” results after first reflow | 61 |
| 6.22 | PCB “twist” results after second reflow | 62 |
| 6.23 | TC 1 temperature vs time | 63 |
| 6.24 | TC 2 temperature vs time | 63 |
| 6.25 | TC 3 temperature vs time | 63 |
| 6.26 | TC 4 temperature vs time | 63 |
| 6.27 | Material science tetrahedron | 65 |

List of Tables

| | | |
|-----|--|----|
| 1.1 | PCB base materials | 2 |
| 2.1 | PCB's classification [3]. | 4 |
| 2.2 | Glass fiber chemical composition | 7 |
| 2.3 | Traditional woven glass fabric styles [8] | 8 |
| 2.4 | Types of conductor material [3]. | 8 |
| 5.1 | Thermal properties standards | 35 |
| 5.2 | Material thermal properties | 36 |
| 6.1 | Glass transition temperature results for the 3 areas | 44 |
| 6.2 | Thermal conductivity of base materials [3] | 45 |
| 6.3 | Specimens mass to obtain decomposition temperature | 46 |
| 6.4 | Results at 3 areas for "x" axis | 50 |
| 6.5 | Results at 3 areas for "y" axis | 52 |
| 6.6 | Results at 3 areas for "z" axis | 54 |
| 6.7 | CTE results at 3 areas | 55 |
| 6.8 | Water absorption results | 58 |
| A.1 | Heat transfer of base materials | 71 |
| B.1 | PCB's dimensions | 72 |
| C.1 | PCB bow results after first reflow | 73 |
| C.2 | PCB bow results after second reflow | 74 |
| D.1 | PCB twist results after first reflow | 75 |
| D.2 | PCB twist results after second reflow | 76 |

Abstract

Printed Circuit Boards (PCB's) are an important component for any electronic device, they can be found in cell phones, computers, tablets, televisions, radios, remote controls, among others. In automotive industry, PCB's are incorporated into the board containing tachometers, water, oil, gasoline levels and all signals displayed on the board. PCB's contain electronic components such as: electric motors, resistors, capacitors, micro-controllers and LED's, just to name a few. To join them, a solder paste of tin, silver and copper alloy (Sn-Ag-Cu) is applied on the PCB surface; then the PCB is processed into a reflow oven at temperature range of 24°C-250°C allowing the solder paste to flow and join the electronic components with the PCB, an operation called "reflow process".

In 2006 the Restriction of Hazardous Substances (RoHS) prohibited the use of lead (Pb) in solder paste, which has a melting temperature around 180°C, whereas lead-free solder pastes have a melting point around 230°C, 30°C-40°C higher than Pb solder paste, this has generated PCB thermo mechanical problems due to the temperature increase at which the material is exposed. Typical problems are related with deformations of the PCB in the reflow process, such as "warpage", which is a deformation along the "z" axis and is accompanied by other phenomena called "bow" and "twist", "bow" is characterized by a curvature of cylindrical shape on both sides of the PCB whereas "twist" is characterized by the elevation of the corners. "Warping", "bow" and "twist" affect subsequent processes such as: assembling engines, micro-controllers, improper electrical tests, false contacts, bending of electronic components and fractures at the interphase between electronic component and the PCB.

The present research work studies the relation between material thermal properties, PCB configurations and reflow conditions with "warping" "bow" and "twist" during the reflow process by the thermal characterization of base materials, deformations measurements and temperature reflow profiles. Thermal properties obtained were: glass transition temperature (Tg), decomposition temperature (Td), Coef-

ficient of thermal expansion (CTE), time to delamination and %water absorption, deformations measurements were obtained on 30 PCB's after exposure. Temperature profiles were obtained by placing thermocouples on the PCB.

Our results suggest that there is a discrepancy between the thermal properties obtained experimentally and data sheet provided by the supplier. PCB "bow" and "twist" data obtained exceeds the values established by the IPC-2221B standard and the temperature profiles met the requirements of the quality control in the company. It is found that there is a mismatch between temperature profiles, it is speculated a relationship with preferential deformations during reflow process.

The present work contribution consists in a whole study of PCB thermo-mechanical performance during reflow process considering material thermal properties, reflow conditions and the influence on PCB deformations.

Chapter 1

Introduction

1.1 What is a Printed Circuit Board?

Printed Circuit Boards (PCB's) are an important component for any electronic device. They can be found in cell phones, computers, tablets, televisions, radios, remote controls, among others [1]. PCB's are used in the automotive industry, they are integrated into the automobiles panel indicators which contains speed, RPM tachometers and temperature, air bags, handbrake and safety signals on the board. Figure 1.1 shows the panel indicators of Sierra truck and figure 1.2 shows a PCB which it is behind the panel of figure 1.1.



Figure 1.1: Sierra GMC indicators panel

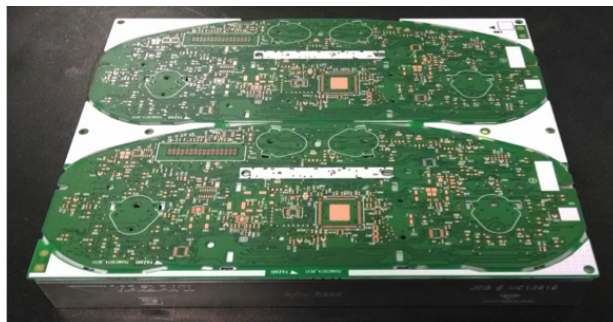


Figure 1.2: Printed Circuit Board

The first PCB's were developed in the 1900's, Albert Hanson described flat foil

conductors laminated to an insulating board in multiple layers, also Thomas Edison experimented with chemical methods of plating conductors in 1904. Arthur Berry in 1923 patented a print and etch method, while Max Schopp in USA obtained a patent. In the 1930's Paul Eisler used a PCB for a radio and the PCB growing was during the World War II due to USA began to use technology on high volume applications [2].

PCB's are made of different materials: resins, reinforcements, conductive material, flame retardants, curing agents and coupling agents [3]. The next section provides a general overview of how a PCB is made.

1.1.1 Base Materials for Printed Circuit Board

Figure 1.3 [4] is schematic representation of cross sectional view and shows how the PCB is made, there are resin/fiberglass layers, copper and fillers. Each material provides some specific property. Table 1.1 lists PCB base materials and their function.

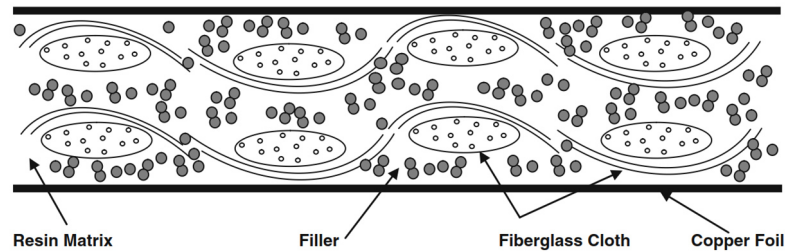


Figure 1.3: PCB configuration

Table 1.1: PCB base materials

| Material | Function |
|-----------------------------|---|
| Reinforcement (glass fiber) | Provide electrical and mechanical properties |
| Resins | Acting to transfer thermal and mechanical loads |
| Coupled agents | Glass fiber and resins interfaces improvement |
| Flame retardants | Reduced flammability |
| Conductor material (copper) | PCB interconnections |
| Cured agents | Polymerization improvement |
| Accelerators | Reduced cured time |
| Fillers | Mechanical properties improvement |

Chapter 2 describes in more detail these base materials, presenting glass fiber styles, resins and conductive material options. To get a PCB functional, it is necessary to place the electronic components, such as: capacitors, resistors, LED's,

motors, displays, micro-controllers among others. The next section explain briefly the electronic components assembly.

1.2 Assembly Process of Printed Circuit Board

A flow chart of electronic components assembly is presented in figure 1.4, “Reflow process” consists to processed the PCB into a oven to joint the electronics components with the PCB by a solder paste.

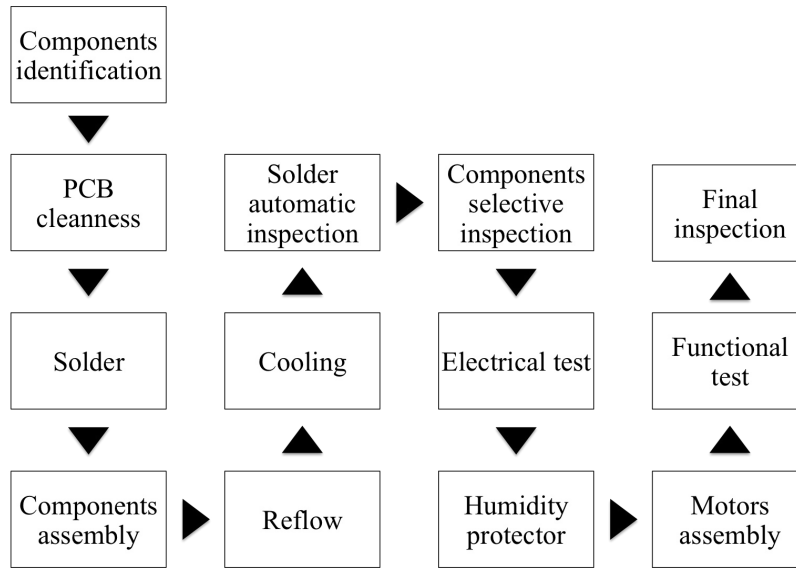


Figure 1.4: PCB’s manufacturing process diagram

During reflow process PCB suffers dimensional changes, causing “bow” and “twist” or PCB “warpage”. “Warpage”, “bow” and “twist” cause PCB defects such as: welding applied incorrectly, component placement incorrectly, false contacts, weak joint between electronic component and PCB. “Warpage” become important since 2006 when the Restriction of Hazardous Substances (ROHS) prohibited the use of lead in solders pastes [5], [6]. Materials have different properties and interacting between them performed different. Chapter 2 presents the based materials for printed circuit board.

Chapter 2

Literature Overview

2.1 PCB's Base Materials

There are many types of PCB's, resin and fiberglass must be considered depending of the conditions to which the materials will be exposed. Table 2.1 shows a PCB classification according with the type of resin and reinforcement.

Table 2.1: PCB's classification [3].

| PCB | Resin | Reinforcement | Flame retardant |
|-------|-----------|--------------------|-----------------|
| FR-2 | Fenólic | Cotton | Yes |
| FR-3 | Epoxy | Cotton | Yes |
| FR-4 | Epoxy | Glass fiber | Yes |
| FR-5 | Epoxy | Glas fiber | Yes |
| FR-6 | Polyester | Glas fiber wave | Yes |
| G-10 | Epoxy | Glass fiber | No |
| CEM-1 | Epoxy | Cotton/Glass fiber | Yes |
| CEM-2 | Epoxy | Cotton/Glass fiber | No |
| CEM-3 | Epoxy | Glass fiber | Yes |
| CEM-4 | Epoxy | Glass fiber | No |
| CRM-5 | Polyester | Glass fiber | Yes |
| CRM-6 | Polyester | Glass fiber | No |
| CRM-7 | Polyester | Glass fiber | Yes |
| CRM-8 | Polyester | Glass fiber | No |

Flame retardant (FR-4) is the PCB most widely used in electronic industry with applications in toys, controls, calculators and computers. In the automotive industry, FR-4 is used in automobiles panel indicator, clocks, LCD's, alarms, among others electronics devices incorporated into the vehicle. According with table 2.1 FR-4 is composed of epoxy resin and glass fiber as a reinforcement. Next sections provides

in more detail these materials.

2.1.1 Resins Systems

Epoxy resins are the most efficient systems used for PCB's due to the combination of good physical, mechanical and electrical properties with it's low cost fabrication compared to high-performance resins systems. Epoxy resins systems are classified as: difunctional, tetra-functional and multifunctional. The prefix "di", "tetra" and "multi" refers to the number of epoxy groups at the end of the molecular chain [7].

Difunctional Epoxy Resin

Bisphenol-A and epichlorohydrin reaction is the most common epoxy resin systems for PCB's. Bisphenol-A brominated provides flame retardancy. The reaction is schematically shown in figure 2.1.

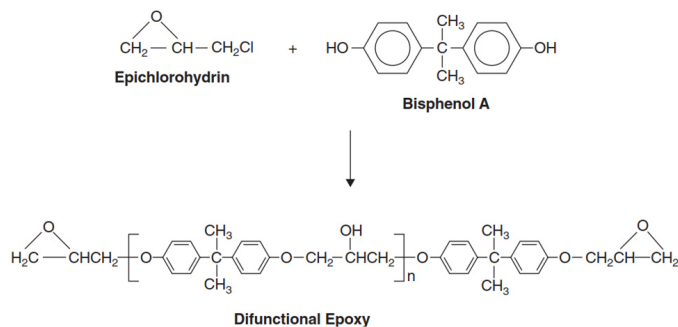


Figure 2.1: Difunctional epoxy resin reaction

When the increase of flame retardancy becomes important, tetrabromobisphenol-A is added in the reaction as figure 2.2 shows, this is another system of difunctional epoxy resin called brominated epoxy resin doped.

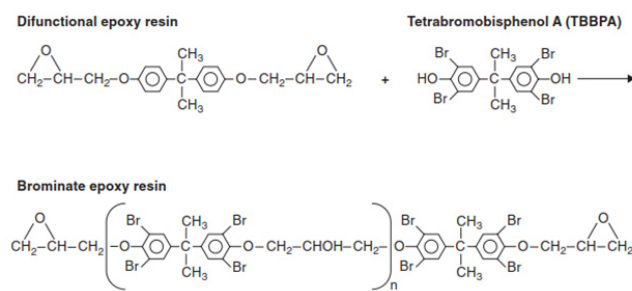


Figure 2.2: Brominated difunctional epoxy resin reaction

Epoxy resin molecular weight depends of the group repetitions at the center of the molecule and final properties depends on: molecular weight, curing agents, glass transition temperature (Tg) and decomposition temperature (Td).

Tetra and Multifunctional Epoxy Resins

Two or more epoxy functional groups per molecule increases higher glass transition temperatures and improve physical and thermal properties. These epoxy resins systems are classified based on glass transition temperature ranges, 125°C-145°C, 150°C-165°C and above 170°C. There are epoxy resins systems with glass transition temperatures above 190°C, which has better properties, but they are expensive. Figures 2.3 and 2.4 are examples of these type of epoxy resins systems.

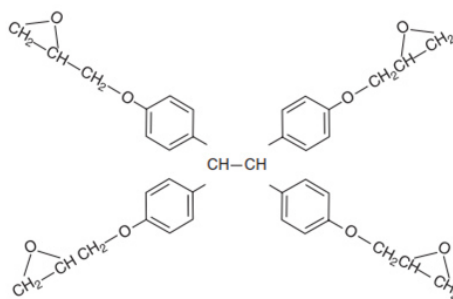


Figure 2.3: Tetrafunctional epoxy resin

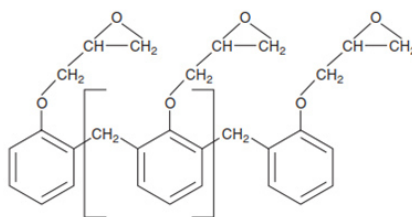


Figure 2.4: Multifunctional phenol novolac epoxy resin

2.1.2 Reinforcements

The reinforcement most used for PCB's is fiberglass due to presents a good combination of electrical and mechanical properties. Glass fiber types are related with their chemical composition as table 2.2 shows. The use of woven glass fibers in PCB substrates dates back to the 1960s where they were used a high performance replacement for paper reinforcement. Woven glass fiber provided an ideal reinforcement to

Table 2.2: Glass fiber chemical composition

| Elements | Style E | Style NE | Style S |
|----------------------------------|----------|----------|---------|
| Silicon dioxide | 52-56 | 52-56 | 64-66 |
| Calcium oxide | 16-25 | 0-10 | 0-0.3 |
| Aluminum oxide | 12-16 | 10-15 | 24-26 |
| Boron oxide | 5-10 | 15-20 | - |
| Sodium oxide and Potassium oxide | 0-2 | 0-1 | 0-0.3 |
| Magnesium oxide | 0-5 | 0-5 | 9-11 |
| Iron oxide | 0.05-0.4 | 0-0.3 | 0-0.3 |
| Titanium oxide | 0-0.8 | 0.5-5 | - |
| Fluorides | 0-0.1 | - | - |

complement the properties of epoxy resin systems which were being rapidly deployed in electronics [8]. However, the most widely used as base material is “E” glass fiber, offering good mechanical and chemical electrical properties for a reasonable cost.

Glass fiber is fabricated in different “styles” as figures 2.5a, 2.5b and 2.5c shows, which are 1080, 2116 and 7628 styles respectively and they are the most commonly used for PCB's. Depending of the PCB thickness the number of layers of the style must be selected.

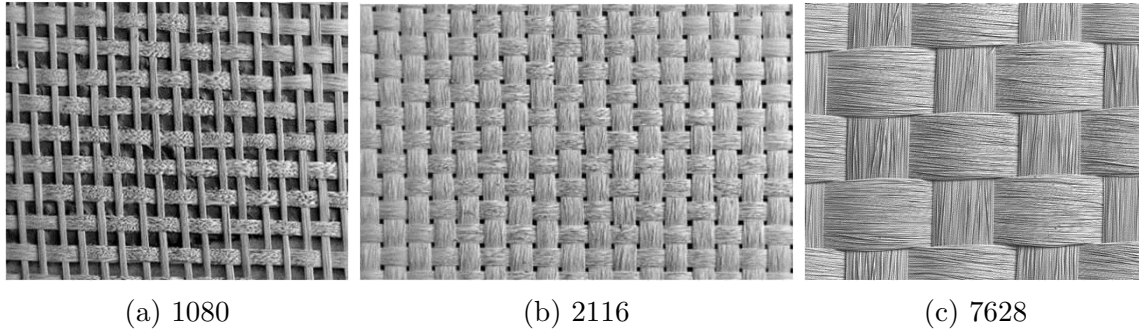


Figure 2.5: Glass fiber styles

Table 2.3 shows the traditional arrangements available [8].

Table 2.3: Traditional woven glass fabric styles [8]

| Style | Glass thickness (mm) | Weight (gsm) | Threads per cm |
|-------|----------------------|--------------|----------------|
| 7628 | 0.17 | 203 | 17.3 x 12.2 |
| 2116 | 0.095 | 104 | 23.6 x 22.8 |
| 2125 | 0.09 | 87 | 15.7 x 15.4 |
| 2113 | 0.079 | 78 | 23.6 x 22.0 |
| 1080 | 0.05 | 47 | 23.6 x 18.5 |
| 106 | 0.033 | 24 | 22.0 x 22.0 |

In the future PCB base materials will no doubt utilize even better fibers and resins and will incorporate entirely new materials, including those on the nano scale. We are indebted to the researches and developers worldwide who continue to advance our knowledge and produce ever more advanced and functional materials to transform the designers dreams into reality [8].

2.1.3 Conductive Material

The main conductive material used in PCB's is copper. Table 2.4 shows the different grades of copper.

Table 2.4: Types of conductor material [3].

| Grade | Foil Description |
|-------|--|
| 1 | Standard electrodeposited (STD-Type E) |
| 2 | High-ductility electrodeposited (HD-Type E) |
| 3 | High-temperature elongation electrodeposited (HTE -Type E) |
| 4 | Annealed electrodeposited (ANN-Type E) |
| 5 | As rolled-wrought (AR-Type W) |
| 6 | Light cold rolled-wrought (LCR-Type W) |
| 7 | Annealed-wrough (ANN-Type W) |
| 8 | As rolled-wrough low-temperature annealable (LTA-Type W) |
| 9 | Nickel, standard electrodeposited |
| 10 | Electrodeposited low temperature annelable (LTA-Type E) |
| 11 | Electrodeposited annealable (A-Type E) |

The most used is electro deposited grade 1 and grade 3. They are produced by electrochemical process where copper is first dissolved in a sulfuric acid solution. Copper sulfate/acid solution is then used to electroplate copper. Grade 3 commonly refers to the elongation at high temperatures, so it is a constituent for multilayer printed circuit boards. The increase in ductility at elevated temperatures provides resistance circuit when thermal stresses are generated and expands in the “z” axis. As a fabrication process improvement there are surface treatments to obtain good adhesion, some of them are described [3].

1. Bonding treatment: coatings of zinc, nickel or brass are introduced. Helps to prevent heat and chemical degradation copper links with the resin during manufacturing process. These coatings typically increase the thickness and color variation.
2. Thermal barriers: A coating of zinc, nickel, or brass is usually applied over the nodules. This coating can prevent thermal or chemical degradation of the foil to resin bond during manufacture of the laminate, the printed circuit, and the circuit assembly. These coatings typically measure several hundred angstroms in thickness and vary in color due to the specific metal-alloy used, although most treatments are brown, gray, or a yellow mustard color.
3. Antioxidants coatings: In contrast to the other coatings, these treatments are virtually always applied to both sides of the foil. Although many of these treatments are chromium based, organic coatings can also be utilized. The primary purpose of these treatments is to prevent oxidation of the copper foil during storage and lamination. These coatings are usually less than 100 angstroms thick and are typically removed by the cleaning, etching, or scrubbing processes normally used at the start of printed circuit manufacturing processes.
4. Coupled agents: The use of coupling agents, primarily silanes such as those used to promote fiberglass to resin adhesion, can also be used on copper foils. These coupling agents can improve the chemical bond between the foil and the resin system and can also be used to help prevent oxidation or contamination.

Resins system, glass fibers and copper layers are incorporated together to form a PCB, depending of customers requirements the systems resin, thickness of glass fiber and copper layer are selected, next section provide a brief explanation of how a PCB is fabricated.

2.2 PCB Fabrication

The first step is coating a resin system onto the woven fiberglass cloth. Rolls of fiberglass cloth are run through equipment called treaters. The fiberglass cloth is drawn through a pan containing the resin system and then precise metering rolls help control thickness, as figure 2.6 shows.

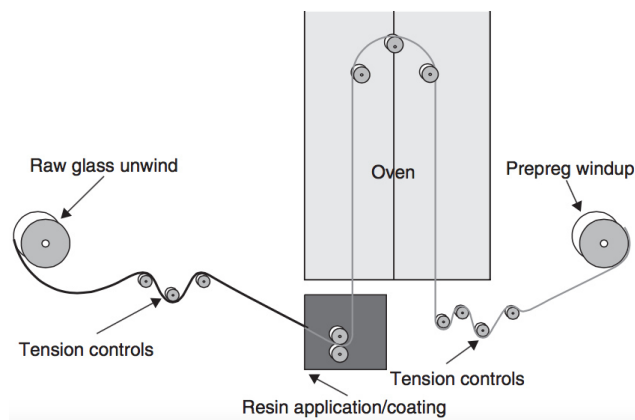


Figure 2.6: “Treating” fiberglass cloth with resin

Next the cloth is pulled through a series of heating zones, which utilize forced air convection, infrared heating, or a combination of the two. In the first set of zones, solvent used to carry the resin system components is evaporated off. Subsequent zones are dedicated to partially curing the resin system. Finally, the prepreg is rewound into rolls or cut into sheets.

Control of the resin/glass ratio, the degree of cure of the resin and cleanliness are critical. Prepregs are stored in temperature and humidity controlled environments. Temperature affect the degree of cure of the resin and therefore its performance in laminate or multilayer circuit pressing. Moisture can affect the performance of many curing agents and accelerators, the performance of the resin system during lamination, humidity it also important to control during prepreg storage. Absorbed moisture that becomes trapped during lamination cycles can also lead to blisters or delaminations within the laminate or multilayer circuit.

Once prepregs are done, they are combined with the desired copper foils to make the finished laminate. Materials are laid up in the proper sequence to produce the desired thickness forming stacks, these stacks are loaded into lamination presses, where pressure, temperature and vacuum are applied, as figure 2.7 shows. Control of the temperature rise during lamination will provide the desired amount of resin flow, while control of the cool down rate can impact warp and twist [3].

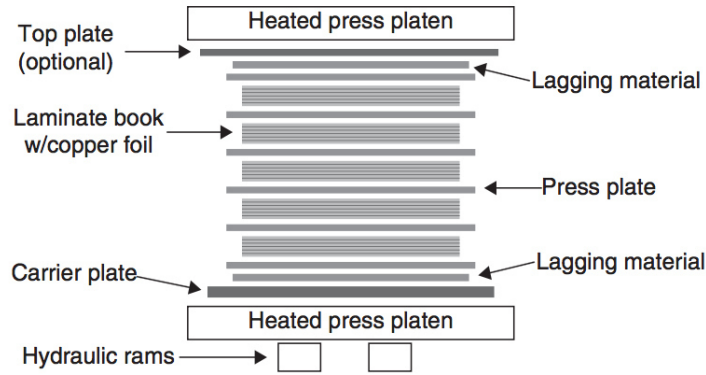


Figure 2.7: Laminate pressing

After laminates are finished next step is to print electronic designs on their surface, also drilling and protection surface are applied ready to incorporate the electronics components by a reflow process, which is described in the next section.

2.3 Reflow Process

PCB's are processed in a reflow oven in figure 2.8 to joint electronic components with PCB by tin-silver-copper (Sn-Ag-Cu) solder paste application, it has 2.95 m of length and the temperature range is from room temperature to 280°C, the average time of reflow process is five minutes.



Figure 2.8: Reflow oven

During reflow process the PCB travels through nine stages, 1 to 5 are preheating stages, 6 and 7 are heating stages and 8 and 9 are cooling stages, as shown in figure 2.9.

At 6 and 7 stages it is important to reach 250°C to ensure the solder paste welding and get the joint between electronic components and PCB [9]. Let's explain briefly

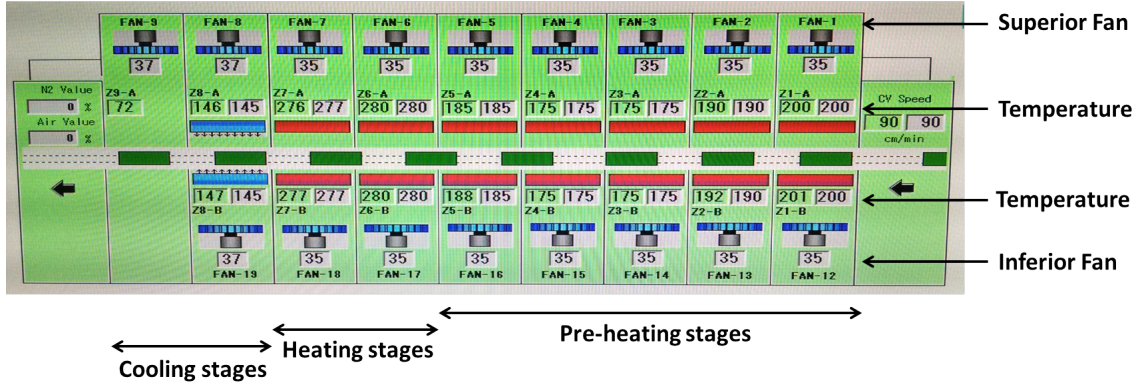


Figure 2.9: Reflow oven stages

lead free solder paste.

Lead-free solder paste

In 2006 RoHS prohibited the use of lead (Pb) [10] on solder pastes the use of lead-free solder pastes began. Pb-based solders were used for jewelry and making bonds between metals including the ancient pipes and aqueducts. Nowadays Sn-based solder alloys have replaced Pb-bearing solders in most applications, but replacing the Pb with Sn was no sufficient for solder joints, so alloying elements such as Cu and Ag to make Sn-Ag-Cu (SAC) alloys have brought performance necessary to meet requirements. Figure 2.10 (a) shows the phase diagram of the lead free solder, there are several invariant reactions. Fortunately, the ternary eutectic of primary interest, consisting of $\beta - Sn$, Ag_3Sn , and Cu_6Sn_5 phases, exists at the Sn-rich corner. Because Al_3Sn and Cu_6Sn_5 phases are thermodynamically independent phases, a reduced ternary diagram consisting of $\beta - Sn$, Ag_3Sn , and Cu_6Sn_5 , can be constructed, meaning that other binary phases do not need to be included in the phase equilibrium considerations at the Sn-rich corner [11].

Figure 2.10 (b) shows this corner in the established diagram, which displays the liquidus surface projected in a Cartesian plot where x-and y-axis represent the Cu and Ag concentration, respectively, with scales that are not the same. The liquidus surfaces merge at one point where the eutectic reaction occurs at 220°C approximately.

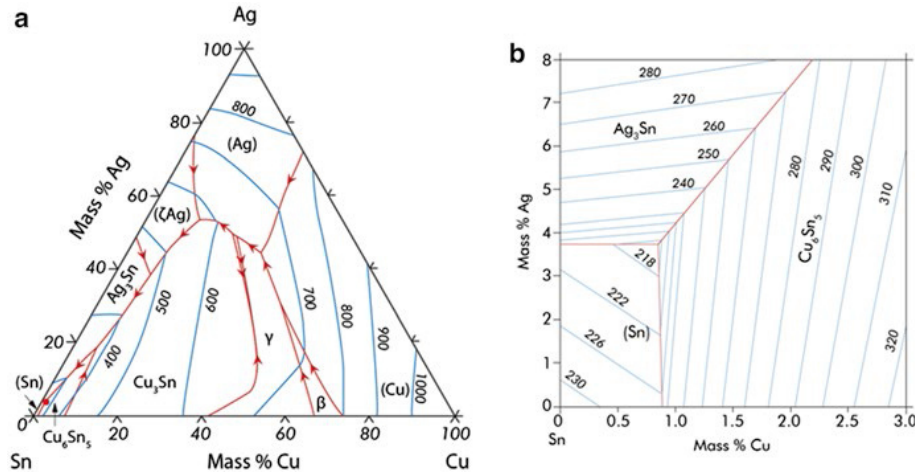


Figure 2.10: Sn-Ag-Cu Solder paste phase diagram [11]

On the other hand the conventional solder paste used before is composed basically of tin and lead (Sn-Pb) which has a melting temperature of 180°C as figure 2.11 shows.

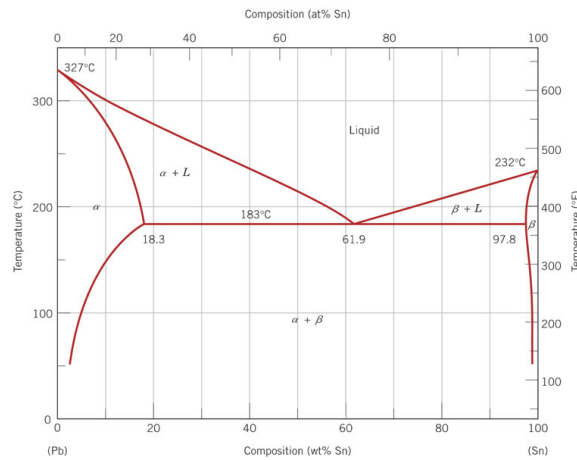


Figure 2.11: Sn-Pb Solder paste phase diagram

The drawback is that lead-free solder paste requires 35°C- 40°C above the melting temperature of the conventional welding resulting the development and implementation of materials that will withstand higher temperatures.

After reflow process there are cooling area as shown in figure 2.12. The cooling area has three stages, depending on the type of PCB and the side which it's processing is the exposure time for cooling, typically cooling time is 40 seconds. First and second stages are at 24°C and third stage at 13°C; fans are installed through the cooling area to accelerate air flow on the PCB cooling.



Figure 2.12: Cooling area

PCB's has components on both sides, so the PCB is processed twice in the reflow oven. Once 2 sides are processed, electrical and functionality tests are performed, also motors and micro-controller are included on the PCB, finally the PCB is stored.

During reflow process there are different failures due to PCB deformations, it has been reported failures due to PCB "warpage" [12], [13]. Pecht and co-authors studied the fracture resistance of welding and ceramic capacitors [14], figure 2.13 is a schematic representation of joint fracture between PCB and capacitor due to "warpage".

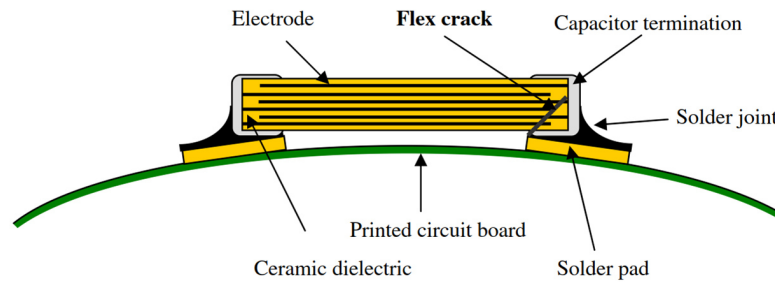


Figure 2.13: PCB's Electronic components failure due to PCB "warpage"

Another example is shown in figure 2.14, which is a capacitor where total fracture is observed. Due to components failures by PCB "warpage", Finite Element Analysis (FEA) models and simulations were developed to predict thermo-mechanical performance of PCB and electronic components; Xueren and co-authors [15] worked on the thermo-mechanical prediction of Ball Grid Array (BGA) by finite element analysis, also experimental methods were performed to compare it with simulations.

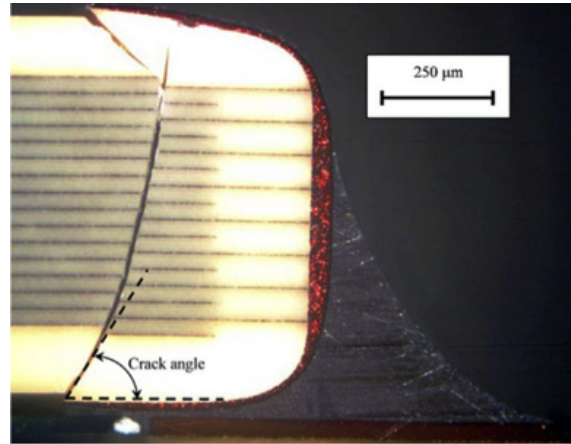


Figure 2.14: Capacitor failure due to PCB “warpage”

Material thermal properties mismatch play an important role during reflow process, thermal conductivity of common FR-4 epoxy resin systems is $0.2\text{--}0.34\text{ W}/(\text{m}^\circ\text{K})$, whereas the thermal conductivity of the fiber glass is lower than that of PCB FR-4 epoxy systems ($0.02\text{--}0.04\text{ W}/(\text{m}^\circ\text{K})$). This mismatch can limit the heat transfer [16], [17], there are other thermal properties that must be considered, such as: glass transition temperature, decomposition temperature, time to delamination, coefficient of thermal expansion, water absorption among others. Engineers must consider material thermal properties when a PCB is designed, the knowledge about material properties becomes an important factor for PCB reliability during the process. Next section provides an overview of material thermal properties.

2.4 Thermal Properties of PCB Materials

2.4.1 Glass Transition Temperature

Glass transition temperatures of typical PCB materials used in the electronic industry varies from 115°C to about 260°C [18]. Glass transition temperature (T_g) has been the most common property used to classify FR-4 base materials. T_g is the temperature at which a polymer starts to change from a rigid state to a “glassy state”. The material is not in a liquid state when it is above the T_g , it is a temperature at which physical changes take place due to the weakening of molecular bonds within the material. It is important to understand T_g since the properties of base materials are different above T_g than below T_g , as the temperature increases, more of the bonds become weakened until for all practical purposes, all relevant bonds are affected. T_g of a resin system has several important implications in thermal

expansion and the degree of cure of the resin system [3].

Figure 2.15 is a schematic presentation to determine glass transition temperature, which consists in draw two parallel lines, one under the transition zone and the other above the transition, identifying the midpoint and intersecting with “x” axis, the glass transition temperature is obtained [19].

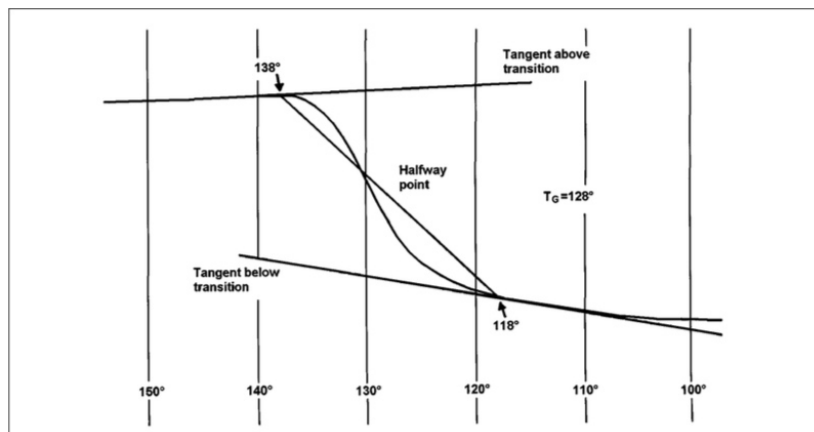


Figure 2.15: Schematic representation to obtain T_g [19]

Several properties change as the T_g is exceeded, including the rate at which a material expands vs. temperature. Young's modulus also decreases significantly as T_g is exceeded [20].

2.4.2 Decomposition Temperature

The material is heated at certain temperature, the resin system will begin to decompose. The chemical bonds will begin to break down and volatile components will be driven off, reducing the mass of the sample. The decomposition temperature (T_d), describes the point at which this process occurs. Traditional T_d is where 5 percent of the original mass is lost to decomposition. 5 percent is a very large number when multilayer PCB reliability is considered, however the reliability of traditional FR-4 becomes important when exhibits 1.5-3 percent of weight loss. This level of decomposition can compromise long-term reliability or result in defects such as delamination during assembly, particularly if multiple assembly cycles or rework cycles are performed, when a material is tested for decomposition temperature 2% and 5% is recorded. Temperatures with lower levels of decomposition are important particularly for lead-free assembly [3].

Figure 2.16 shows the curves for two FR-4 materials.

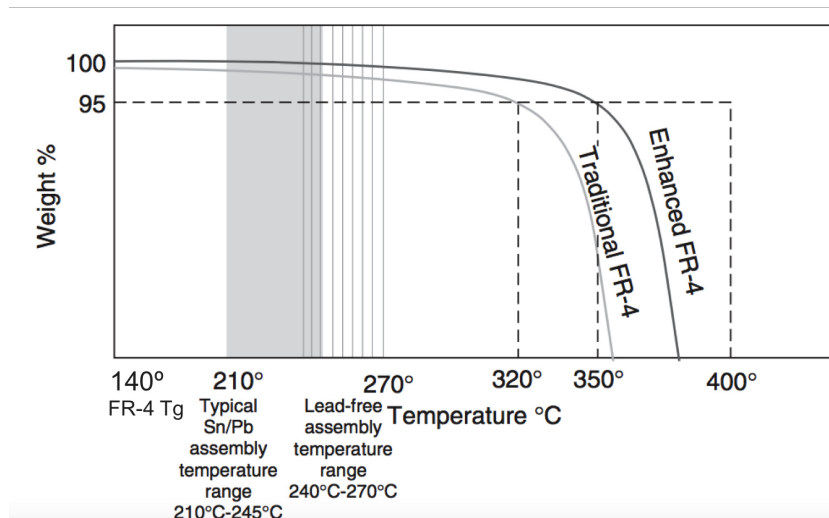


Figure 2.16: Decomposition temperature chart for different FR-4 types

The traditional FR-4 with 140°C of Tg material has a decomposition temperature of 320°C by the 5 percent weight loss definition. The enhanced FR-4 has a decomposition temperature of 350°C by the 5 percent weight loss definition. Many standard high-Tg FR-4 materials actually have decomposition temperatures in the range of 290-310°C, while the 140°C Tg FR-4 materials generally have slightly higher Td values. In figure 2.16 the shaded regions indicate the peak temperature ranges for standard tin-lead assembly and lead-free assembly [3].

Resin decomposition can result in adhesion loss and delamination. A 5% level of decomposition is severe, and intermediate levels are important for assessing reliability since peak temperatures in lead-free assembly can reach onset points of decomposition [20].

2.4.3 Coefficient of Thermal Expansion

Coefficient of thermal expansion (CTE) of printed circuit boards have a great deal of influence on the reliability of solder joints in microelectronic packages [21]. CTE values above Tg are much higher than below Tg. Reflow process temperatures result in more total expansion for a given material. However, several mature lead-free compatible materials incorporate inorganic fillers that reduce CTE values [20].

A specimen thickness vs specimen temperature chart is recorded to calculate CTE. Figure 2.17 is a schematic representation to obtain CTE, two values are determined, CTE below glass transition temperature and CTE above glass transition temperature.

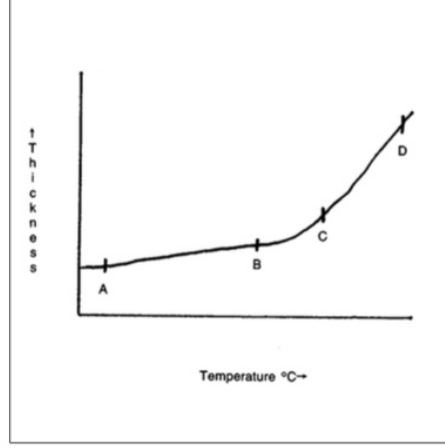


Figure 2.17: Representation to obtain coefficient of thermal expansion

CTE below glass transition temperature is obtained selecting two points before the transition, in this case are “A” and “B”, they represents two temperatures (T_A and T_B) and their thicknesses (L_A and L_B), values are substituted in the formula 2.1:

$$CTE_{(A-B)} = \frac{(L_B - L_A)10^6}{L_0(T_B - T_A)} \quad (2.1)$$

Where:

- T_A = temperature at “A” point in figure. 2.17.
- T_B = temperature at “B” point in figure. 2.17.
- L_0 = thickness or initial length.
- L_A = thickness or specimen length at point “A” in figure 2.17.
- L_B = thickness or specimen length at point “B” in figure 2.17.

CTE above transition temperature is obtained selecting two points after the transition, which are “C” and “D”, temperatures (T_C and T_D) and their thicknesses (L_C and L_D) are substituted in the formula 2.2:

$$CTE_{(C-D)} = \frac{(L_D - L_C)10^6}{L_0(T_D - T_C)} \quad (2.2)$$

Where:

- T_C = temperature at “C” in figure 2.17.

- T_D = temperature at “D” in figure 2.17.
- L_0 = thickness or initial length.
- L_C = thickness or specimen length at point “C” in figure 2.17.
- L_D = thickness or specimen length at point “D” in figure 2.17.

CTE are determined in “x”, “y” and “z” axes, figure 2.18 shows the PCB directions. Coefficient of thermal expansion units are part per million over Celsius degrees (ppm/°C).

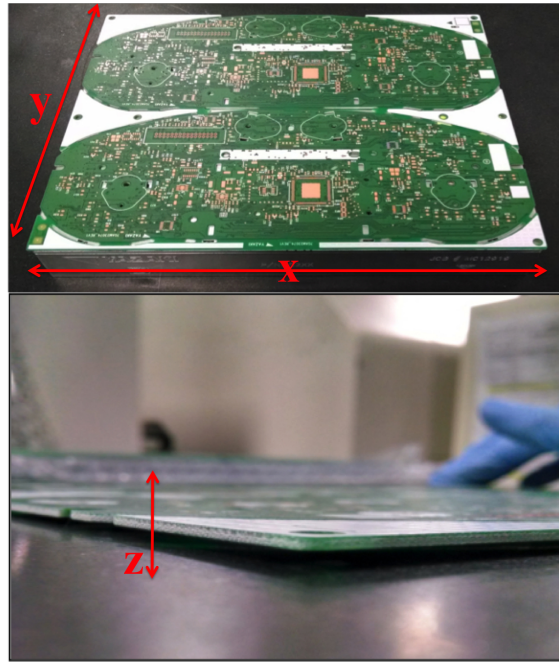


Figure 2.18: CTE axes

2.4.4 Time to delamination

Time to delamination is when the PCB presents slip between glass fiber and epoxy resin layers due to temperature exposures, this phenomena is common in polymer matrix composite materials reinforced with fibers. We must remember that the PCB is made of laminated resin and glass fibers, so analyze this property is important. The test involves measuring the change in specimen thickness versus temperature increase, specimens are heating from room temperature to 260°C at 20°C/min. Once 260°C is reached, an isothermal is applied for 10 minutes, if the specimen shows no change in thickness during isotherm, is a guarantee that the material will not

present delaminations in reflow process, which peak temperature is $245^{\circ}\text{C} \pm 5^{\circ}\text{C}$, that's the main reason of tested the specimen at 260°C . However, if exhibits a change in thickness means that the glass fibers are detaching of the epoxy resin. These detachments are characterized by raising the glass fibers generating an increase in specimen thickness represented as peaks in figure 2.19.

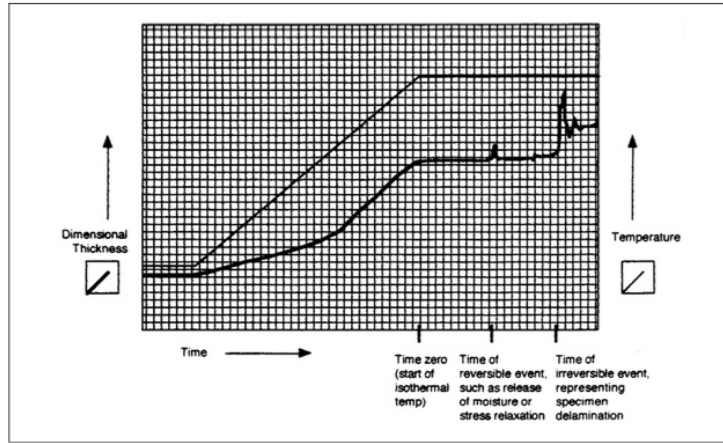


Figure 2.19: Representation to obtain time to delamination

First peaks correspond to a reversible change such as humidity, stresses release or relaxation and second characteristic peaks represent irreversible changes of PCB delamination [22]. Thermal expansion and moisture absorption can also influence results. In multilayer PCB's, the treatment of the internal copper surfaces is also critical [20].

2.4.5 Water Absorption

The reliability of printed circuit boards laminates is influenced by the presence of moisture, which can be present in the epoxy glass prepreg absorbed during the wet processes in the fabrication of the PCB's or diffuse into the PCB during storage. Moisture may reside in the resins, resin/glass interfaces and microcracks or voids due to defects causing internal shorts through metal migration and changes in dimensional stability [23], it can generate failure mechanisms during electronic components assembly, also reduces the glass transition temperature and increases the dielectric constant [24], leading to a reduction in circuit switching speeds and an increase in propagation delay times [25]. Percentage of water absorption determines how sensitive the material it is when is exposed to moisture. Vapor pressure of water is much higher at lead-free assembly temperatures. Absorbed moisture can volatilize during thermal cycling and cause voiding or delamination. PCBs that initially pass lead-free assembly testing may exhibit defects after storage in an uncontrolled environment, as a result of moisture absorption. This should be considered when evaluating materials and PCB designs [20].

Percentage of water absorption was obtained by the formula 2.3:

$$\%Water = \frac{M_{water} - M_{oven}}{M_{oven}} \cdot (100) \quad (2.3)$$

Where:

- M_{water} = mass after 24 hours distilled water immersion.
- M_{oven} = mass after oven.

Materials thermal properties described above are important factor for PCB reliability, also plays an important role for “bow” and “twist” phenomena, which it will describe in next section.

2.5 “Bow” and “Twist”

“Bow” is defined as any deviation of the material to the plane on which is supported, is characterized by an elevation in cylindrical form in one area of the material [26] as shown in figure 2.20. “Twist” refers to the elevation of a rectangular PCB generated parallel or diagonally to the supporting surface, typically it is characterized by elevated corners [26], figure 2.21 is an example of “twist”. “Warping” is any deformation caused by thermo-mechanical stresses causing deformations at different PCB areas.

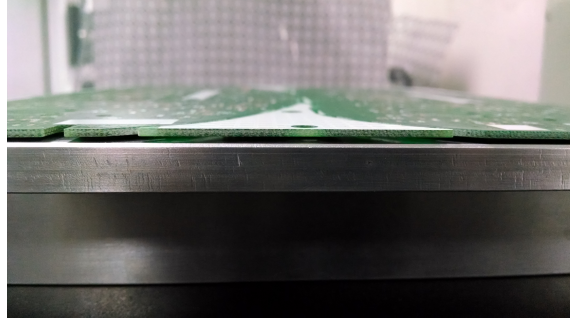


Figure 2.20: “Bow”

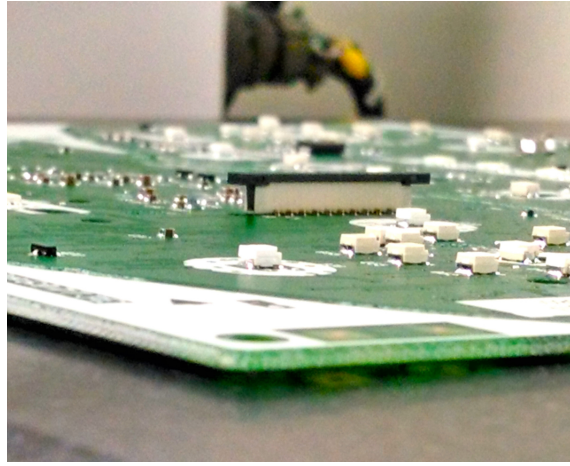


Figure 2.21: “Twist”

“Bow” and “twist” becomes important for electronic industry, companies related with PCB’s must take in consideration this phenomena and has to be measure, very precisely method is the “Shadow Moiré technique” and consist in diffraction patterns by light beams which hit the PCB and deformations are recorded in the order of micrometers, another approach more practical and easily to performed is the method described in IPC-TM-650 test methods manual 2.4.22c Bow and Twist (Percentage) standard [26].

Formulas 2.4 and 2.5 are used to obtain “bow” and “twist” percentage, respectively:

$$\%Bow = \frac{R}{L} \cdot (100) \quad (2.4)$$

$$\%Twist = \frac{R}{2D} \cdot (100) \quad (2.5)$$

Where:

- *Bow*: percentage of “bow”.

- R : distance between plane and PCB surface at each side.
- L : PCB length.
- $Twist$: percentage of “twist”.
- R : distance between plane and PCB corners.
- D : PCB diagonal length.

First step is identify the PCB corners and PCB sides. Figure 2.22 represents the identification of areas that will be measured to obtain “bow” and “twist”.

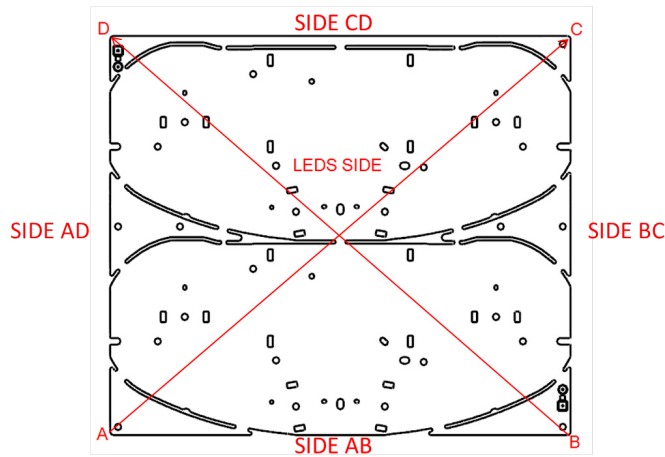


Figure 2.22: “bow” y “twist” areas identification

Figure 2.23 shows a schematic representation of PCB thickness, PCB diagonals and PCB sides lengths. The first step is to get the lengths of the sides AB, BC, CD and DA as figure 2.23a shows, the lengths of the diagonals AC and BD in figure 2.23b and the thicknesses of the PCB corners in 2.23c.

Vernier is used to lengths and diagonales measurements and a micrometer for thicknesses. After PCB first reflow process, heights are measured, which is the distance between the flat surface and PCB surface, the measurement is made at the midpoint of each side PCB, as can be seen in figure 2.24.

This procedure is performed for each side of the PCB, obtaining four measurements of “ R ” values are substitute in equation 2.4 described above and the result for %bow is obtained.

For % twist, the procedure is the same, the height is obtained at PCB corners, as shown in figure 2.25, then the PCB thickness is subtracted from height to obtain the free space between the PCB and the surface.

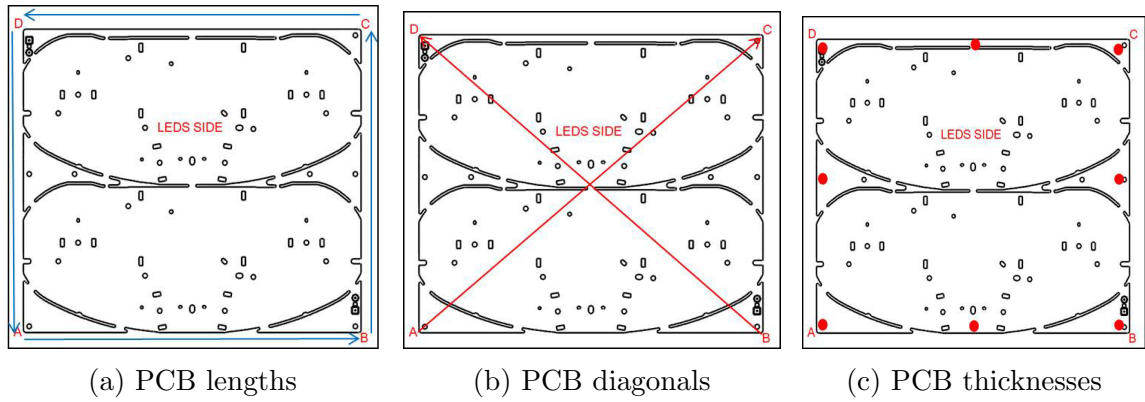


Figure 2.23: PCB schematic representation of thickness, diagonals and lengths

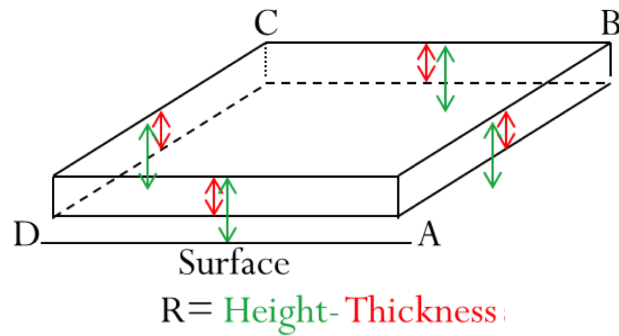


Figure 2.24: PCB schematic representation to obtain % of bow

Electronic industry grows, however, there is a few literature about PCB's performance and it's necessary to generate experts in the field [27]. According with material properties overview, the materials involved to fabricated PCB's and the process. Chapter 3 present the state of the art about the study of PCB materials, reflow oven and the latest advances related with PCB's and it's processing.

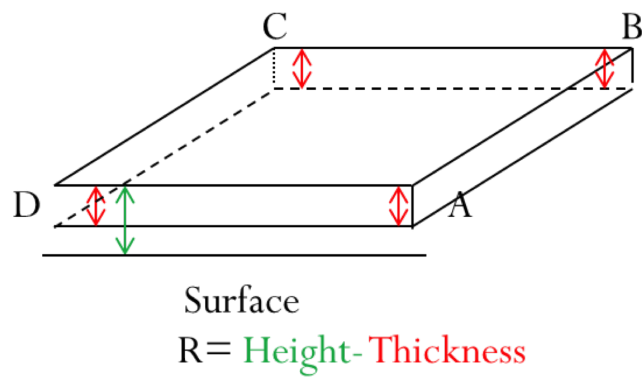


Figure 2.25: Schematic representation to obtain % of twist

Chapter 3

State of the Art

Thermo-mechanical distortions during reflow process are present in the PCB's. Trough the years researches has been development studies to understand the interaction that occurs with materials and the processes. Literature reviewed can be divided in 3 topics:

- Materials properties
- Reflow oven
- Warpage

This chapter presents the literature reviewed in order to establish objectives, hypothesis and experimental plan as well.

3.1 Material Properties

K. Azar in collaboration with AT&T Bell Laboratories [28] obtained thermal conductivities “k” at each single PCB layers by infrared microscopy, concluding the mismatch between glass fiber layers and Cu pattern. Yujun [29] in 2004 developed a thermal stresses model under constant loads considering a orthotropic material, also a “Shadow Moiré” technique was performed to validate his results, deformations caused by thermal stresses were obtained experimentally and finally results were validated by finite element analysis. H. Qi, M. Pecht and co-authors in 2005 [30] compared high Tg FR-4 and Polyimide (PI) printed circuit boards in relation with life time welding joints, where PI board provides a better solder joint durability. In the same year, Ehrler [31], investigated the response of two different epoxies resins and concluded they were not suitable for thermal stresses during reflow process.

Ravikumar Sanapala in 2008 [32], characterized materials before and after temperature exposures. Pradeep Lall [18] in 2012 based on Sanapala's research, studied PCB's glass transition temperature changes. Jie Zhang and co-authors studied the degradation of epoxy grupos of three different epoxy resin base material for Printed Circuits Boards by TMA, DSC, although they established a correlation of curing and thermal properties [33]. R. Polanský and coauthors in 2014 [16], determined fiberglass and resin strength by thermal analysis performing tests under Tg values, but increasing time exposure from 170°C to 200°C.

Shuo Xiao and co authors improve the thermal conductivity in the through-thickness direction, it is possible to design vias into PCB's. based on previous researches, they placed a copper plate under the PCB and it was the best [34].

Ercan M. Dede and co-authors studied the anisotropic thermal conductivity in PCB'S, where the flow of heat is manipulated through the informed layout of circuit board electrothermal traces. Three representative circuit board configurations are considered. Experimental results are verified through simulations explaining the functionality of the heat flow control concept [35]. Also Michal B. and co-workers [36] improved the heat dissipation using alternative materials.

Recently Eva and co-authors [37] tested materials to establish long-term reliability data for PWB materiales for use in applications that require 20+ years of operational life under different thermal conditions, teste were based on a 5000 hour expected operation life of the electronic product. Therefore there is a need to determine the dielectric breakdown/degradation of the composite PCB material and mechanical structure over time and temperature for mission critical applications.

3.2 Reflow Oven Process

The reflow oven is an important factor of PCB thermo-mechanical performance PCB. David C. Whalley in 1991 developed a reflow process simulation in two reflow ovens adding the coefficient of convective heat transfer in the cooling stages [47]. Motorola developed finite element analysis to validate their experimental results [38]. Farhad Sarvar [48] developed a transient state model varying PCB thermal properties, also generated experimental data to validate his model. David C. Whalley improved his previous work considering radiation and thermal conductivity to predict PCB temperatures at each reflow oven stages [49]. Motohiro and co-authors [50] studied the heat convection coefficient "h" with a new design of fans modifying exit air diameters. Etsuko Iwasaki [51] optimized the heating, cooling, air collection

and oxygen-nitrogen control systems by the improvement of holes configuration at exit air flow, creating a stable air flow and a uniform heat transfer heat through the PCB. Balázs Illés and co-authors [52] studied the thermal distribution analyzing the convection heat transfer coefficient “h”, also performed a simulation in 3D showing the uniformity of heat flow on the PCB.

Since 2010, most of the research is focus in thermo-mechanical prediction by simulation models. Yasutada Nakagawa and Ryohei Yokoyama [53] in 2011 designed a PCB to reduce “warpage” based on composite materials deformation theory [54], [55]. Fuchs, G. Pinter and M. Tonjec [56] in 2012 compared mechanical behavior of materials layers obtained experimentally with mechanical properties of each layer by finite element analysis. Jabin Zhang and Paolo Emilio Bagnoli in 2013 [57] proposed a methodology of PCB thermal analysis. Eric Monier-Vinard and co-authors [58] in 2014 compared thermal performance of multilayers model with materials properties such as: heat transfer coefficient, thermal conductivities and number of layers.

3.3 Warpage

One of the first researches on “warpage” was developed by C.P Yeh in collaboration with Motorola [38], where they approach a finite element model with 4 techniques: ultrasonic, lasers, projection speckle and shadow moiré, PCB thermo-mechanical simulations has been developed to predict deformations during reflow process [39], [40], [41]. Then Yarom Polsky [42] in 1998 developed a model based on thermoelastic theory considering material properties and temperature conditions, also “Shadow Moiré” technique was developed to validate his model [43], which measurements are based on light beams diffractions, also complementary researches reported measurements by strain gauges [44]. Chi-Hui Chien and co-authors in 2006 [45] investigated micro-controllers “warpage” used in PCB’s establishing a relationship between results and percentage of moisture absorption at different temperatures. Sung-Jun and co-authors studied film warpage demonstrating the warpage dependence of temperature with viscoelastic properties modification [46].

3.4 Summary

According with the literature reviewed, it can be concluded that PCB reliability depends on:

- PCB material properties

- Reflow process

Researches of PCB materials properties involves thermal and mechanical properties in some cases, but mostly of the researches studied thermal properties, such as glass transition temperature, decomposition temperature, coefficient of thermal expansion, time to delamination, the interaction between them when the material is exposed at high temperatures.

Reflow process literature is an important factor to understand the thermo-mechanical performance of the PCB, because is the process which provides the thermal energy and the responsible that the PCB suffers dimensional changes, causing “warpage”, studied focused on temperatures distributions through PCB, the homogeneity of the flow air at the different stages, it has been studied the mechanism of heat transfer, conduction, convection and radiation obtaining the coefficients of each mechanism. As a consequence there are many studies of “warpage” which consist in the measurements of PCB distortions, different techniques have been used since basic gauge tools and the use of refracted light beams or better known as Shadow Moiré, although different researches were originated such as warpage prediction by finite element analysis, incorporating material properties and conditions of process.

The customers expect from their PCB suppliers that the materials are fully characterized and that qualification samples are available immediately. In many cases, the process recommendations given to the PCB manufacturers are very generic (like FR4) and data sheet are different in comparison with real values, it's important to ensure the reliability of base material properties [59].

It is important to mention that all the literature reviewed reported values after thermal exposure, the experimental proposed in this research is taking in consideration no reflow process for specimens tested.

Chapter 4

Motivation, General Objective, Specific Objectives and Hypothesis

4.1 Motivation

Technological progress is growing in innovation and development of new materials, this growth is reflected in sophisticated electronic devices such as: smartphones, electronic tablets, computers, radar systems, televisions, stereos, GPS systems in automobiles among others, PCB's are used in all of them. Companies are interested in PCB's research to get a better understanding of their performance [27], [60].

Automotive industry represents an important source of revenues and profits in the world. In 2015 the Center for Automotive Research (CAR) reported there are 7 million jobs in the private sector. Additionally, 14 companies are focused on vehicles development and research such as: engineering development, design, business facilities and manufacturing operations [61]. Automotive requirements are becoming more sophisticated causing the development of new technologies and the client preferences are the main reason for companies to develop ideas and incorporate them to the automobiles. The main areas are: fuel, emissions control, reducing vehicle weight, aerodynamic design, engine improvement, transmission, and alternative materials composition for electronic components [61].

In 2006, RoHS prohibited the use of lead (Pb) [10] on solder pastes which have a melting temperature of 180°C and the use of lead-free solder pastes began, with a melting temperature around 220°C. The drawback is that the latter requires 35°C-40°C above the melting temperature of the conventional welding resulting in the development and implementation of materials that will withstand higher manufacturing temperatures.

New challenges emerged in quality, production, and cost reduction areas [20]. As an example of this situation, Soonwan Chung and co-authors [62] developed a “warpage prediction” during reflow process for flexible PCB’s used in smartphones. The upcoming release of apple Inc’s iphone 6s series, which will feature Force Touch Tehcnology, is expected to drive demand for flexible PCB’s [63].

The world market for PCB’s reached an estimated \$60.2 billion value in 2014 [64]. Besides, according to IPC’s World PCB Production Report for the year 2014, production growth in China, Thailand and Vietnam [64]. During PCB assembly there is an estimated 2.4% of scrap due to causes related with “warpage”, “bow” and “twist”, representing an important lost of money. Based on the state of the art consulted an insufficient knowledge in the field is detected. Thus the motivation for this research work is to know materials behavior when PCB’s are processed. Additionally, the knowledge generated will help for any new models in future years [65].

4.2 General Objective

Generate new technological and scientific knowledge about the thermo-mechanical performance of FR-4 laminates for PCB’s during manufacturing in the reflow process by studying the interplay among thermal properties, PCB distortions and the main process variables.

4.3 Specific Objectives

1. Elucidate the relationship between the measured thermal properties of the FR4-PCB composite material with the thermo-mechanical behavior observed in the particular process studied.
2. Characterize and analyze PCB warpage in relation to material properties and process conditions, by performing systematic measurements of bow and twist after the first and second reflow processes.
3. Provide a basic conceptual framework that includes material properties, process conditions and thermo-mechanical behavior for the overall reflow process.

4.4 Hypothesis

It is possible to analyze the PCB reflow process in an integral manner in order to generate a better understanding of the thermo-mechanical behavior of the FR4-laminates and the interplay of the material properties and process conditions. This strategy can generate new knowledge about the predominant factors associated to bow and twist distortions that characterize the defect known as warpage, allowing to eventually generate better strategies to control or avoid this condition.

Chapter 5

Experimental Methodology

Based on literature review and the objectives established, an experimental plan was established as figure 5.1 shows.

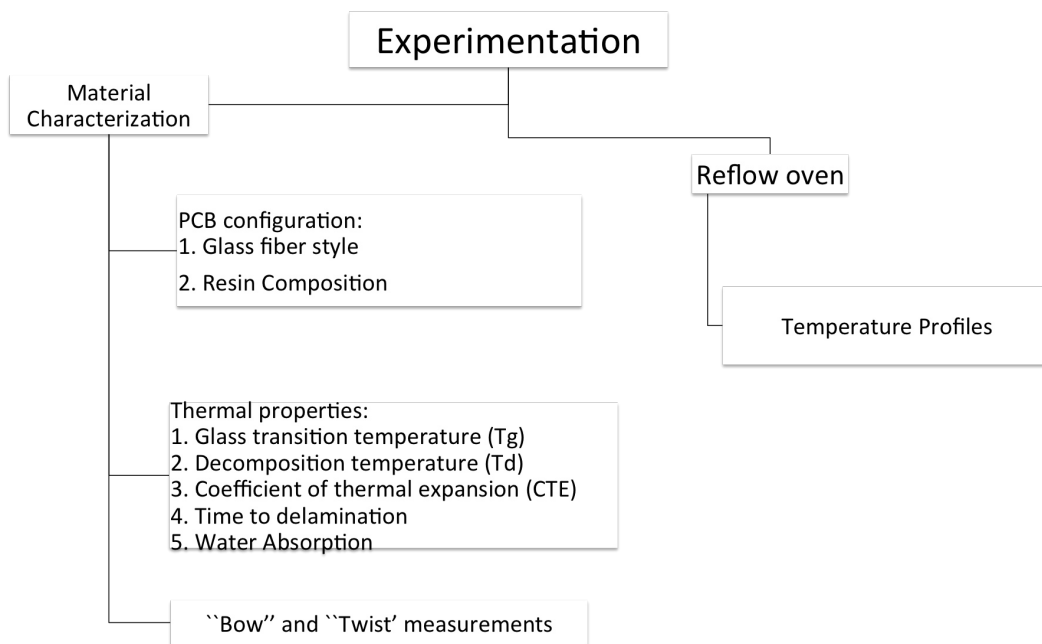


Figure 5.1: Experimental procedure

5.1 Material Characterization

5.1.1 PCB configuration

The PCB material was provided by STACY CORPORATION, is a FR-4 laminate with seven layers of glass fiber, 40% brominated epoxy resin and two copper layers at the top and the bottom, as figure 5.2 shows.

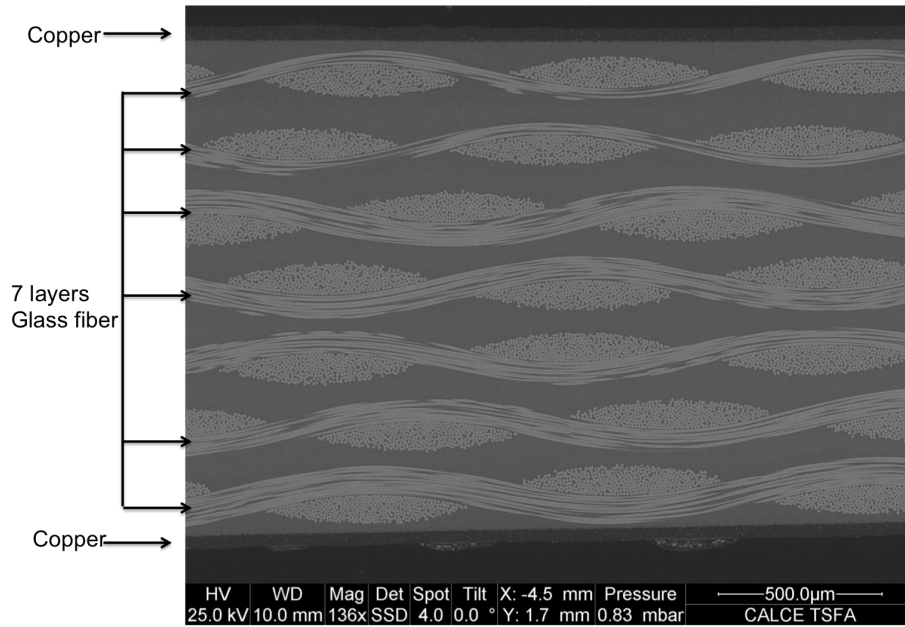


Figure 5.2: PCB cross sectional view showing PCB layers configuration

5.1.2 Thermal Properties

The properties of interest in this research are: glass transition temperature (T_g), decomposition temperature (T_d), coefficient of thermal expansion (CTE), time to delamination and water absorption. Table 5.1 shows the thermal properties studied, the IPC standard and the equipment used. Specimens were prepared and tested according to IPC-TM-650, three specimens were taken from top, middle and bottom PCB areas as shown in figure 5.3, in order to know if there is a variation in thermal properties depending on the PCB area.

Table 5.1: Thermal properties standards

| Property | Units | Standard | Equipment |
|--------------------------------------|--------|---------------------|----------------|
| Glass transition temperature | °C | IPC-TM-650 2.4.25 | DSC |
| Decomposition temperature | °C | IPC-TM-650 4.24.6 | TGA |
| Coefficient of thermal expansion “z” | ppm/°C | IPC-TM-650 2.4.24.5 | TMA |
| Coefficient of thermal expansion “x” | ppm/°C | IPC-TM-650 2.4.24.5 | TMA |
| Coefficient of thermal expansion “y” | ppm/°C | IPC-TM-650 2.4.24.5 | TMA |
| Time to delamination | min | IPC-TM-650 2.4.24.1 | TMA |
| Water absorption | % | IPC-TM-650 2.6.2.1 | Balance |
| Bow and twist | % | IPC-TM-650 2.4.22 c | Gages, vernier |

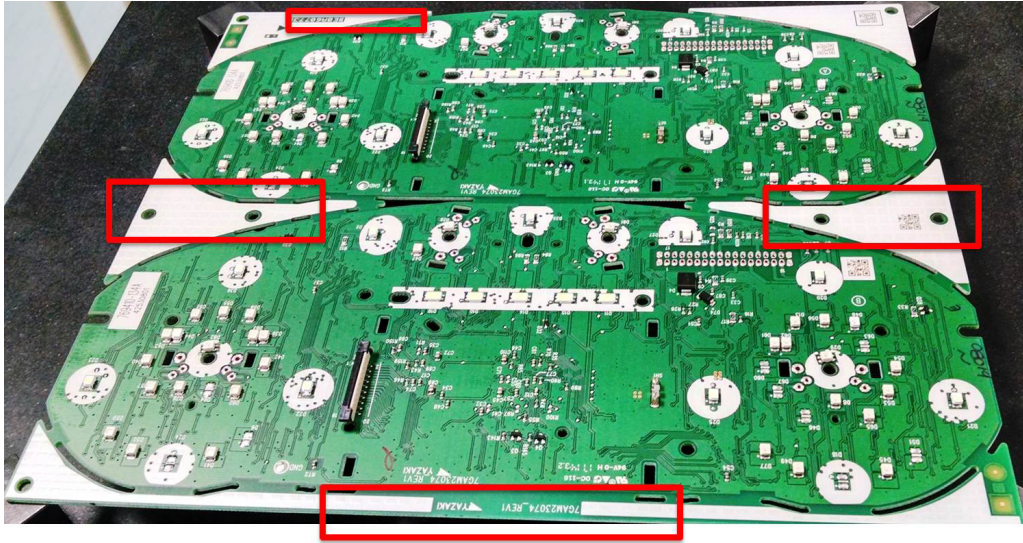


Figure 5.3: Specimens at different areas of PCB

The nominal material properties according to the supplier data sheet are listed in table 5.2.

All specimens were preheated in the oven shown in figure 5.4 at 105°C for two hours to eliminate water or moisture.

Table 5.2: Material thermal properties

| Property | Units | Value |
|---|--------|-------|
| Glass transition temperature | °C | 140 |
| Decomposition temperature | °C | 310 |
| Coefficient of thermal expansion before Tg | ppm/°C | 64 |
| Coefficient of thermal expansion after Tg | ppm/°C | 300 |
| % Coefficient of thermal expansion 50°C-260°C | % | 4.5 |
| Time to delamination | min | 15 |
| Water Absorption | % | 0.15 |



Figure 5.4: Preheating oven

Glass Transition Temperature (T_g)

The equipment used was a Netzsch DSC pegasus F4 shown in figure 5.5. Specimens were prepared based on the IPC-TM-650 2.4.25 standard [19]. The test was run in an argon atmosphere, the temperature range was from 24°C to 170°C at 20°C/min of heating rate. Results were obtained by the procedure established in IPC-TM-650 2.4.25 standard [19]. Figure 5.10 shows the specimens mounted to obtain glass transition temperature, the dimensions were 4 mm x 2 mm and 22 mg approximately of weight.

Decomposition Temperature

Specimens were prepared based on the IPC-TM-650 4.24.6 standard [66]. The Dynamic Mechanical Analysis (DMA) apparatus shown in figure 5.7 was used.

The test was run in an argon atmosphere from 24°C to 550°C at a heating rate

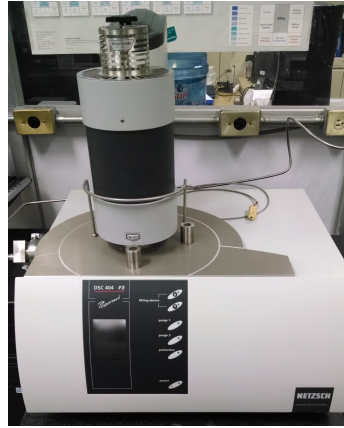


Figure 5.5: DSC Netzch pegasus

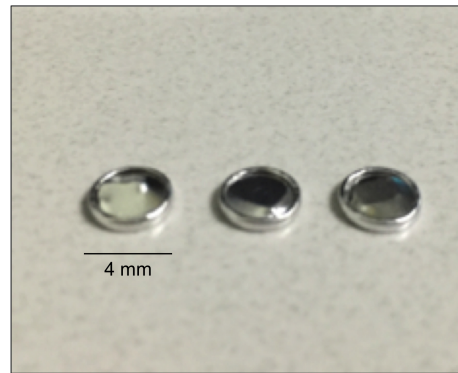


Figure 5.6: Specimens to obtain glass transition temperature

of $10^{\circ}\text{C}/\text{min}$. Specimen mass vs temperature charts were recorded, T_d is reached when the specimen loses 5% of its initial mass. Figure 5.8 shows decomposition temperature specimens, dimensions and weight are the same as for T_g specimens.

Coefficient of Thermal Expansion (CTE)

The thermal expansion coefficient is obtained based on IPC-TM-standard 350-2.4.25.5. The equipment used was a Thermo-mechanical Analyzer (TMA) as figure 5.9 shows.

CTE was obtained in three directions (“x”, “y” and “z”), three specimens were obtained for each zone (top, middle, bottom) of the PCB, obtaining a total of nine specimens, three specimens for the top, three for the middle and three for the bottom. Specimens dimensions were 6.5 mm x 6.5 mm, they were preheated for 1 hour at 105°C , tests were conducted in a nitrogen atmosphere from 30°C to 160°C at a heating rate of $10^{\circ}\text{C}/\text{min}$. Copper was removed from all the specimens as established, then they were identified according with the corresponding axis.



Figure 5.7: Dynamic Mechanical Analysis (DMA)

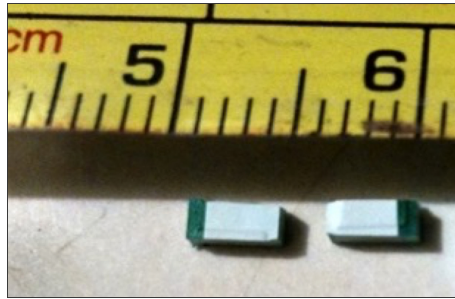


Figure 5.8: Specimens to obtain decomposition temperature

Time to delamination

Time of delamination test was based on IPC-TM -650-2.4.24.1 standard [22], specimens dimensions are 6.5 mm x 6.5 mm, a preheated for 2 hours at 105°C was applied. The test started from room temperature to 260°C at a heating rate of 10°C/min, a isotherm was applied for 10 minutes at 260°C. The delamination time is when a irreversible change in thickness occurs during the isotherm. Dimensions and weight specimens are the same with CTE specimens ones.

Water Absorption

Water absorption test were based on IPC-TM-650 2.6.2.1 [67]. Scales “OMRUS” of figure 5.11a was used. Figure 5.11b shows the specimens were used, specimens dimensions were 2 in x 2 cm and 9.11 gr average weight, then specimens were preheated at 105°C for two hours.

After preheated was completed specimens mass was recorded and immersed in



Figure 5.9: TMA (Thermo Mechanical Analyzer)

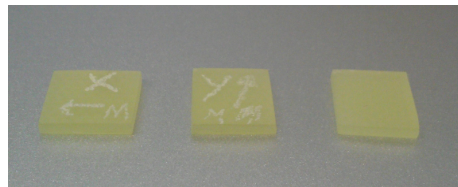


Figure 5.10: Specimens to obtain coefficient of thermal expansion

distilled water for 24 hours. After 24 hours specimens mass was recorded and % of absorption water was obtained by the formula 2.3 explained in Chapter 2.

“Bow” and “twist”

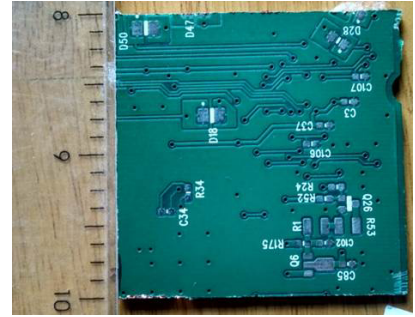
In chapter 2 and 3 it was mentioned that there are different techniques to obtain PCB deformations, “Shadow Moiré” is one of the most precisely technique, however, it was decide to obtained as IPC-TM-650 2.4.22 bow and twist (percentage) standard [26] stated, due to we don’t have the necessary equipment to use Shadow Moire technique, also its expensive, instead data collected approach a good approximation of the PCB deformations with gage devices and measurement instruments.

3 lots were analyzed, 10 PCB per lot, giving a total of 30 PCB’s. Thicknesses, sides and diagonals lengths were measured also they are required to use the formulas of “bow” and “twist” and determine the results.

Chapter 2 explained the formulas to obtain “bow” and “twist”, values of PCB sides, diagonals and thicknesses at each side and each corner are necessary. Vernier and micrometer were used to obtained sides, thicknesses and diagonales measurements, to obtain the deformation of the PCB, the device showed in figure 5.12 measure the height of the PCB from the surface.



(a) Balance



(b) % Absorption water specimens

Figure 5.11: Specimens water absorption performed



Figure 5.12: Device to obtain height of the PCB's

5.2 Reflow Oven

5.2.1 Temperature Profiles

PCB was performed to obtain profiles temperature. Four thermocouples were placed along the PCB in order to collect temperature data, also it was considered to place thermocouples at 1cm from PCB surface to obtain environment temperature and determine if there are a mismatch among PCB areas as figure 5.13.

PCB was exposed to reflow process 5 times and data of temperature vs time was recorded for analysis.

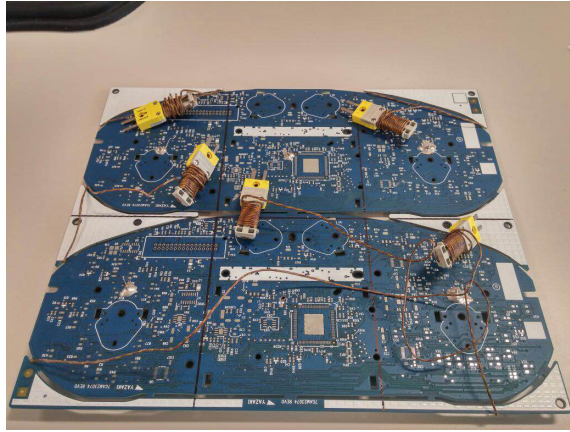


Figure 5.13: PCB to measure oven temperatures

Figure 5.14 is a standard profile temperature, Z1 to Z2 are preheated stages during the first 60 seconds approximately then a isothermal is applied from stage Z3 to the beginning of stage Z6, after the isotherm the peak temperature occurs in Z6 and Z7 during 60 seconds to ensure the melting point of solder paste and finally a cooling rate is applied in Z8 and Z9 stages.

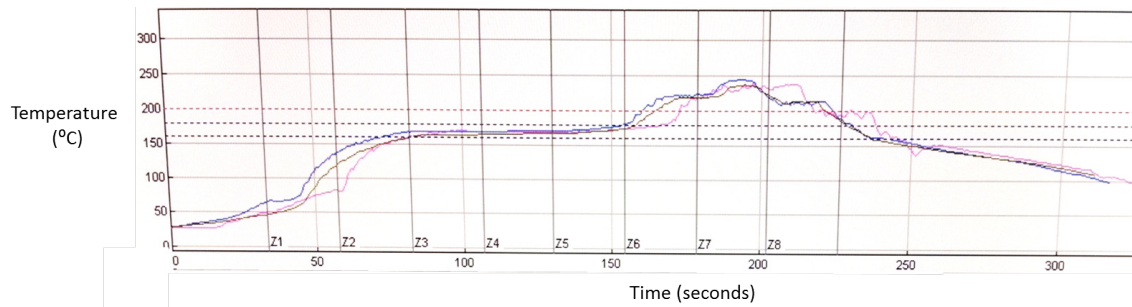


Figure 5.14: Standard PCB reflow process profile

Chapter 6

Results and Discussion

This chapter shows the results obtained as follows:

- Glass transition temperature.
- Decomposition temperature.
- Coefficient of thermal expansion.
- Time to delamination.
- Absorption water.
- % “Bow” and % “twist”.
- Reflow oven.

6.1 Glass Transition Temperature (T_g)

It is important to mention that the specimens were tested before reflow process, no thermal load was applied before, except when the PCB was fabricated. Figure 6.1, figure 6.2 and figure 6.3 represents the results for top, middle and bottom areas, respectively.

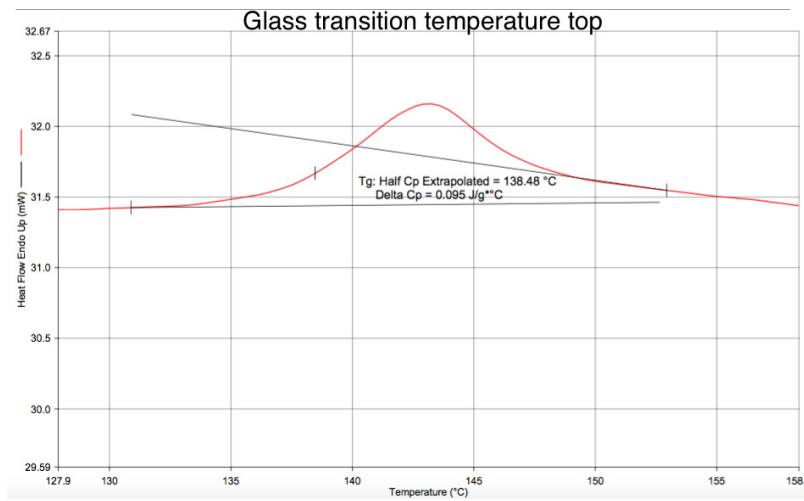


Figure 6.1: Glass transition temperature chart top area

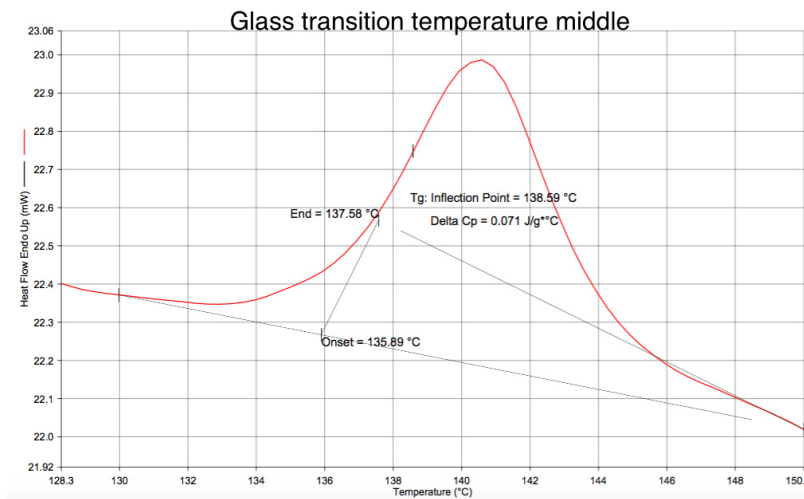


Figure 6.2: Glass transition temperature chart middle area

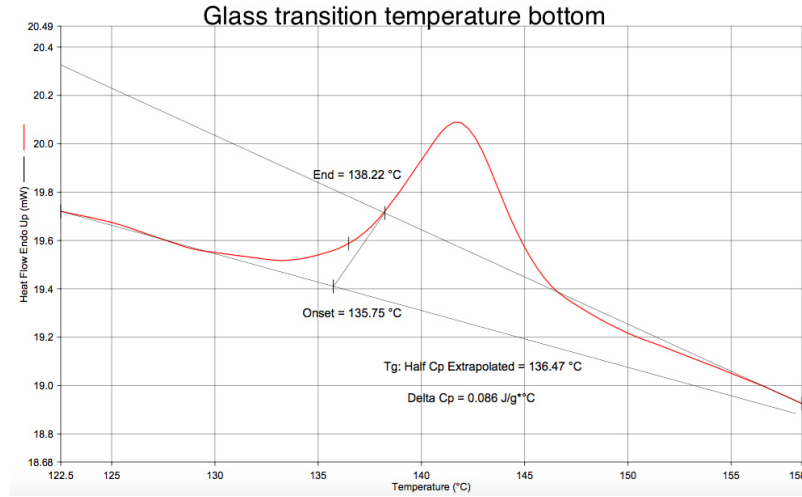


Figure 6.3: Glass transition temperature chart bottom area

Table 6.1 shows the values for the 3 areas.

Table 6.1: Glass transition temperature results for the 3 areas

| Area | Temperature (°C) |
|---------|------------------|
| Top | 138.48 |
| Middle | 138.6 |
| Bottom | 136.47 |
| Average | 137.85 |

There is a reduction of Tg before thermal exposure, at the three areas average value was 137.85°C, values are lower than 140°C, which is the glass transition temperature that data sheet supplier establish. It is speculated that if the material is processed by first and second reflow, this property decrease due to exposure temperature, causing considerable distortions by resin relaxation, exposure temperatures above Tg changes the properties of the laminate, coefficient of thermal expansion and the elastic modulus thus changing the product reliability [68], [69].

Material thermal properties are different at elevated temperatures, “warping” is originated due to thermal properties mismatch during reflow process, thermal conductivity are different between glass fiber, epoxy resin and copper. Table 6.2 shows the thermal conductivity of base materials, the difference between them is evident, glass fiber has the lowest value of thermal conductivity, whereas copper has $401 \frac{W}{m \cdot ^\circ C}$, that means, glass fiber restricted that heat flow and the copper allows the heat transfer with more velocity than glass fiber and epoxy resin.

Table 6.2: Thermal conductivity of base materials [3]

| Material | Thermal Conductivity ($\frac{W}{m \cdot ^\circ C}$) |
|-------------|---|
| Fiber Glass | 0.04 |
| Cobre | 401 |
| Epoxy resin | 0.35 |

If we determined the heat transfer individually considering conduction heat transfer mechanism, values for base materials obtained individually are:

- Copper: 185,605.7 kW
- Epoxy resin: 52.018 kW
- Glass fiber: 6.89 kW

Calculation details are presented in appendix A. According with the results of heat transfer, it is noticeable the difference between glass fiber and copper, glass fiber is a barrier of heat transfer, and the epoxy resin transfer the energy slower than copper.

6.2 Decomposition Temperature (Td)

Decomposition temperature is when the material suffers irreversible changes. 2% and 5% of mass loss is recorded.

Figure 6.4, shows decomposition temperature of the three specimens, “x” axis represents temperature in degrees Celsius ($^{\circ}\text{C}$) and “y” axis the mass loss percentage. Note that the three specimens have a mass loss at 300°C , approximately.

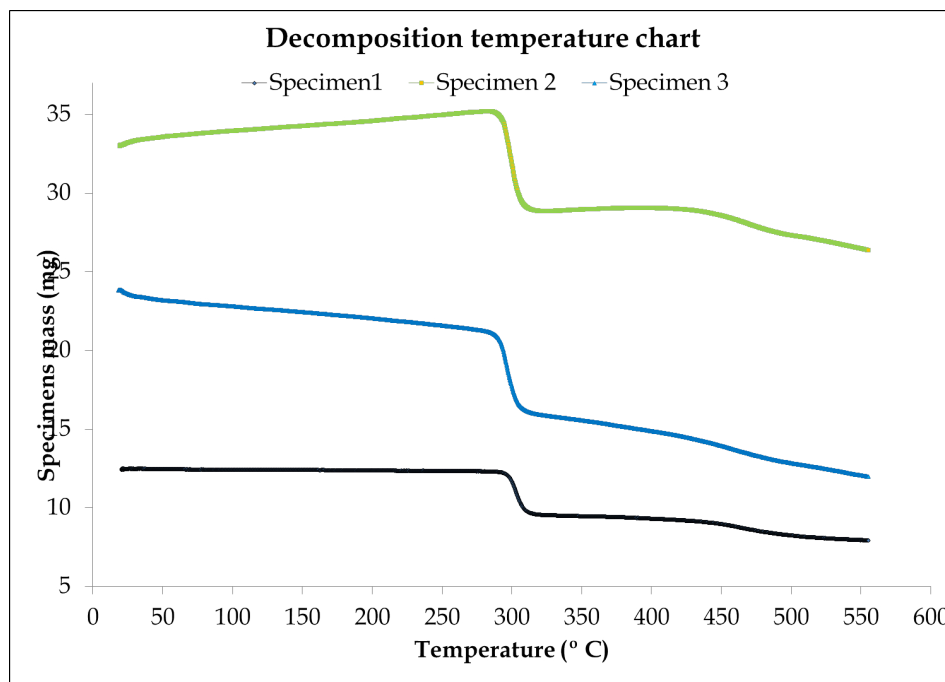


Figure 6.4: Decomposition temperature chart

To obtain more accurate results, specimen 1 and 2 data were fixed where mass loss occurs. Table 6.3 summarized the results.

Table 6.3: Specimens mass to obtain decomposition temperature

| Specimen | Initial mass (gr) | %2 mass lost / temperature ($^{\circ}\text{C}$) | %5 mass lost / temperature ($^{\circ}\text{C}$) |
|----------|-------------------|---|---|
| 1 | 12.43 | 12.18/294.87 | 11.80/299.20 |
| 2 | 33.01 | 32.34/300.28 | 30.72/302.29 |

Figure 6.5 corresponds the specimen 1 mass loss. 2% mass loss is at 294.87°C as the yellow point shows, also in figure 6.5 the red box indicates the 5% of mass loss which is 299.20°C .

Figure 6.6 shows the decomposition temperature of specimen 2. 2% and 5% are presented by yellow point and red box, respectively, which are 300.28°C at 2% and

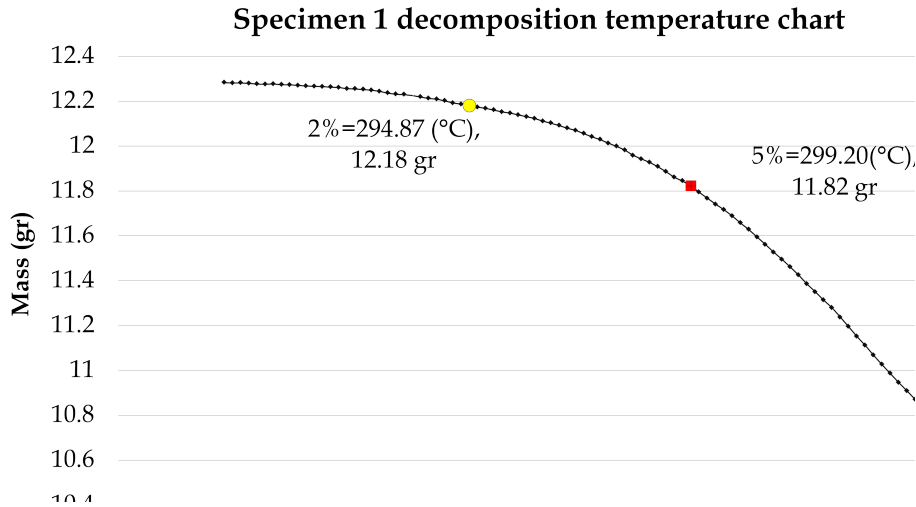


Figure 6.5: Specimen 1 decomposition temperature chart

302.29°C for 5% mass loss.

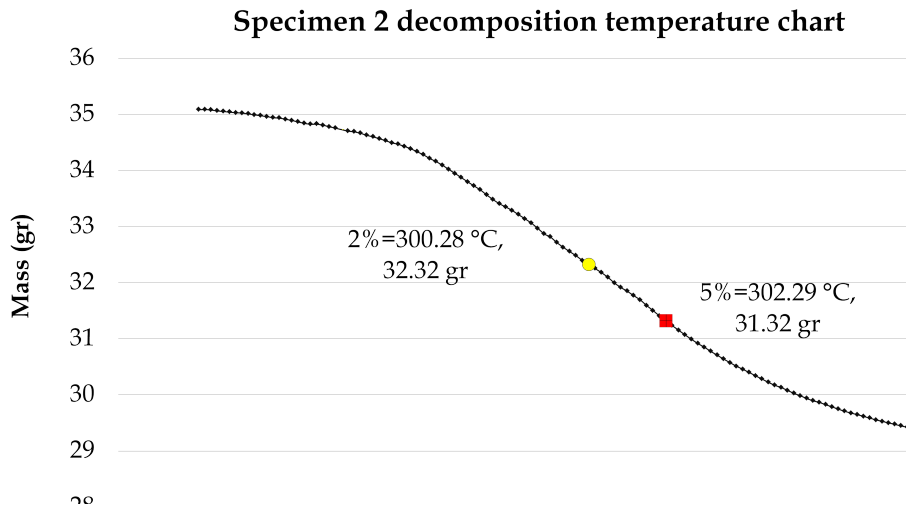


Figure 6.6: Specimen 2 decomposition temperature chart

Decomposition temperature results are lower than the values provided by supplier, there is a decrease of 10°C, decomposition temperature plays an important role, this property tells us the temperature when the material starts to decompose, there are researches which investigate the release of brominated, phenolic compounds when the material reaches certain temperature at different steps of resin decomposition [70]. The process of PCB fabrication becomes important, the process of curing has to be controlled because if the epoxy resin is not fully cured, when the material is exposed in reflow process, there is a probability that the PCB will not complete the process of curing and the resin flux or the decomposition of volatile elements can be pre-

sented. Also no full cured decrease decomposition temperature, in this case if the temperature is lower than traditional temperature (300°C) during reflow process the resin can be suffer a decomposition affecting the reliability of whole product.

6.3 Coefficient of Thermal Expansion

Coefficient of thermal expansion are presented as follows:

- Coefficient of thermal expansion results in the “x” axis.
- Coefficient of thermal expansion results in the “y” axis.
- Coefficient of thermal expansion results in the “z” axis.

6.3.1 Coefficient of Thermal Expansion in the “x” axis

Figure 6.7 shows the results of “x” axis at the top area, the behavior presented is a typical for glass fiber/epoxy resin laminate, change of direction is observed as yellow point marks.

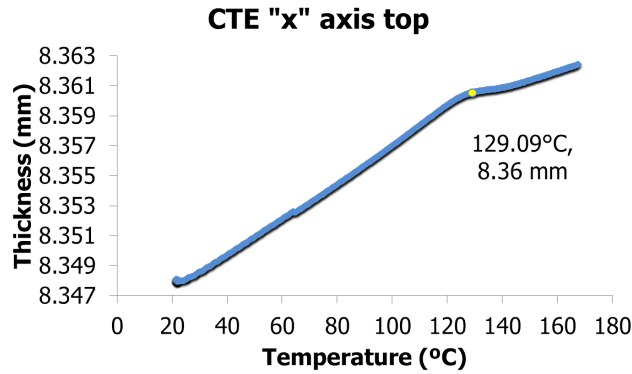


Figure 6.7: Coefficient of thermal expansion “x” axis at top area

Figure 6.8 shows the results of the coefficient of thermal expansion in the axis “x”, but at the middle area. Clearly, the behavior is quite different in comparison with figure 6.7, as yellow point indicates, when temperature approaches to the glass transition a material contraction is observed, then at 140°C the material expansion continues linearly.

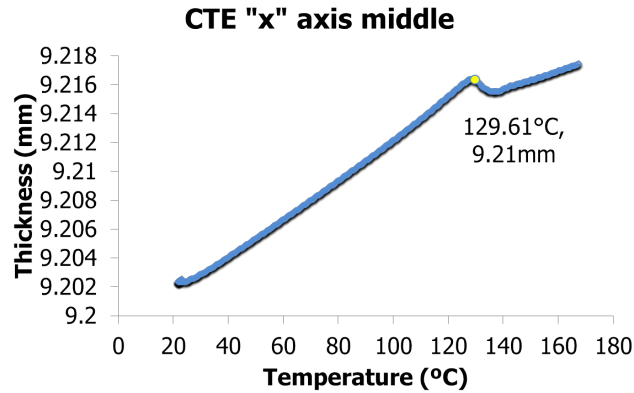


Figure 6.8: Coefficient of thermal expansion “x” axis at middle area

Figure 6.9 shows the results of coefficient of thermal expansion at the bottom. The behavior is similar to the coefficient of thermal expansion of the top area, yellow point indicates the change in specimen thickness at 130.9°C.

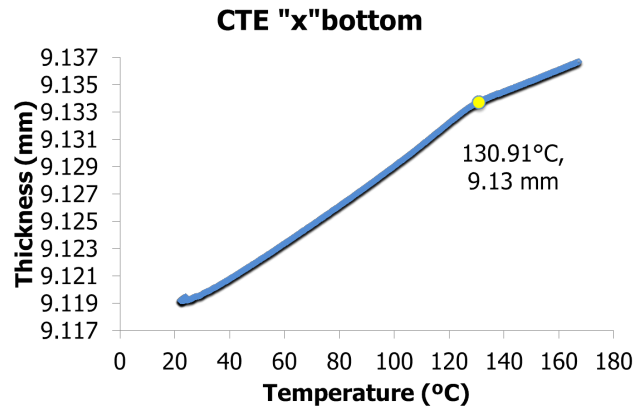


Figure 6.9: Coefficient of thermal expansion “x” axis at bottom area

Mismatch values at middle area in comparison with top and bottom area it is speculate due to a material heterogeneity at the middle, means an inadequate distribution of fiberglass and epoxy resin inducing thermal stress differences between areas, it is believe there a major concentration of epoxy resin than fiberglass, otherwise, the material do not present considerable contractions as shown in figure 6.8.

This change of thickness is due to during the test a force of μN is applied when the specimen reaches a temperature close to the glass transition, the material becomes in a glassy state and with the force applied the material is contracted, this temperature is around 129°C. The contraction observed can cause undesirable epoxy resin flow.

Two coefficients of thermal expansion are obtained, one before and one after the glass transition temperature, two points are selected, before the transition “A” and “B” temperature and thicknesses are recorded and substituted in the formula 2.1:

For the thermal expansion coefficient after the glass transition temperature same procedure is repeated, except that two different points after the transition must be selected. Table 6.4 summarizes “x” axis results, thermal expansion coefficients and % thermal expansion at the three areas are showed.

Table 6.4: Results at 3 areas for “x” axis

| Area | thermal expansion(%) | CTE before Tg (ppm/°C) | CTE after Tg (ppm/°C) |
|--------|----------------------|------------------------|-----------------------|
| Top | 0.17 | 14.81 | 7.12 |
| Middle | 0.16 | 14.90 | 6.92 |
| Bottom | 0.18 | 15.30 | 9.00 |

It is observed bottom area presents an % expansion of 0.18% and the thermal expansion coefficients obtained were 15.30 ppm/°C and 9.00 ppm/°C before and after glass transition temperature, respectively.

Top and middle area values are similar, but the difference between top and bottom area is 0.49ppm /°C for CTE before the glass transition temperature and 1.88 ppm /°C after glass transition temperature.

6.3.2 Coefficient of Thermal Expansion in the “y” axis

Figure 6.10 represented the coefficient thermal expansion at top area in “y” axis, the red point marks a material contraction at 127.75°C close to the glass transition temperature, after tansition the material continue it’s deformation linearly.

The behavior of the coefficient of thermal expansion in the axis “y” at the top is very similar to the coefficient of thermal expansion in the axis “y” in the middle shown in figure 6.11 this contraction occurs at 128.62°C.

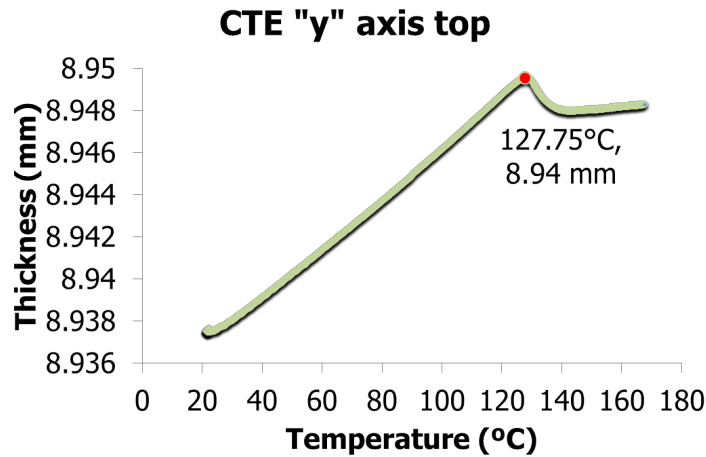


Figure 6.10: Coefficient of thermal expansion “y” axis at top area

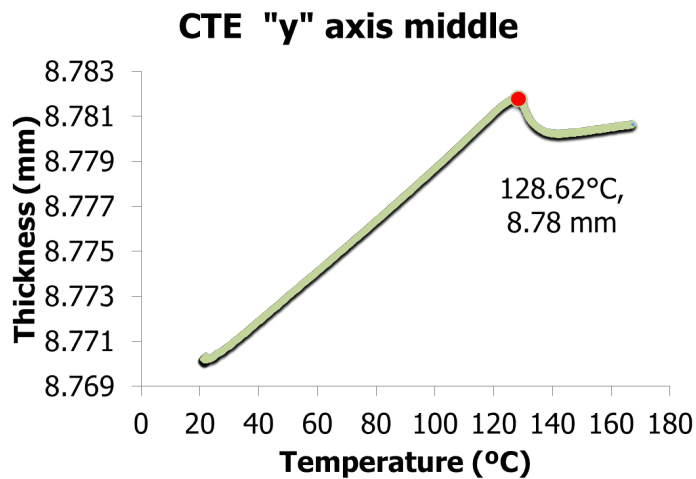


Figure 6.11: Coefficient of thermal expansion “y” axis at middle area

Figure 6.12 represents the results of “y” at the bottom, red point marks the contraction at 130.20°C.

Coefficient of thermal expansion in “y” axis differs between top and middle area with bottom area. Table 6.5 group the results of thermal expansion coefficient percentages and the thermal expansion coefficients in “y” axis for three three areas.

Results suggest that thermal expansion percentage and coefficient of thermal expansion at the bottom area differs significantly compared to the values obtained at the top and middle ones. There is a difference of 0.039% for thermal expansion percentage (0.157205569 to 0.117747654). Coefficient of thermal expansion at the bottom is higher, 7.12 ppm/°C, compared with top and middle area which are 1.53 ppm/°C and 2.11 ppm/°C respectively after glass transition temperature.

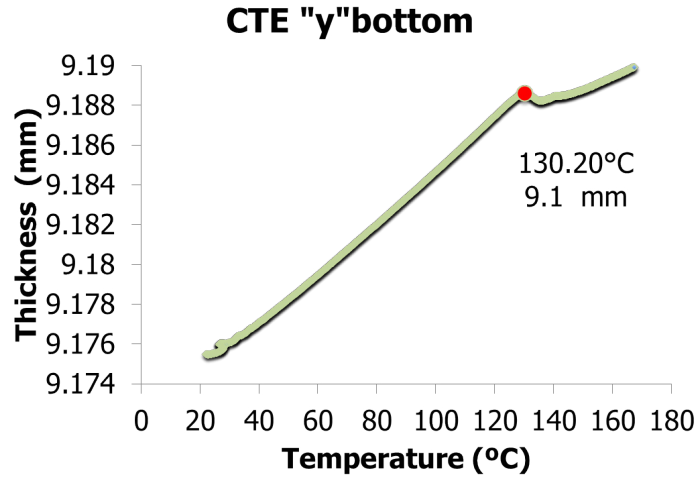


Figure 6.12: Coefficient of thermal expansion “y” axis at bottom area

Table 6.5: Results at 3 areas for “y” axis

| Area | % thermal expansion | CTE before Tg | CTE after Tg |
|--------|---------------------|---------------|--------------|
| Top | 0.119486757 | 13.29 | 1.53 |
| Middle | 0.117747654 | 13.08 | 2.11 |
| Bottom | 0.157205569 | 13.77 | 7.12 |

Also comparing CTE's for “x” and “y” axis, results differs after glass transition temperature, see table 6.5 and table 6.4. The reason of that is because the glass fiber arrangement is not the same, glass fiber styles are fabricated in 2 directions called warp and fill, there are more yarns in one direction than the other one, it is speculated that the axis with higher CTE is the axis with higher fiber glass yarns. Glass fiber restricted the heat flow, there is major concentration of fiber glass in that specific direction, the total heat flow is transfer to the resin and this phenomena cause a thermal stresses by the heat trapped. If there are lower glass fiber, the restriction of heat flow decrease, and the heat flows is transferred more rapidly to the environment.

6.3.3 Coefficient of Thermal Expansion in the “z” axis

In industry, “z” axis is the major concern where deformations are generated and “warpage” is observed. Results of the coefficient of expansion and thermal expansion percentage in “z” axis were analyzed. Figure 6.13 shows the results of the coefficient of thermal expansion in the axis “z” at the top. The behavior is normal according with the standard [71], near the glass transition temperature an expansion is observed at 136.79°C, after transition material continues it's lineal expansion at a similar rate before the glass transition temperature.

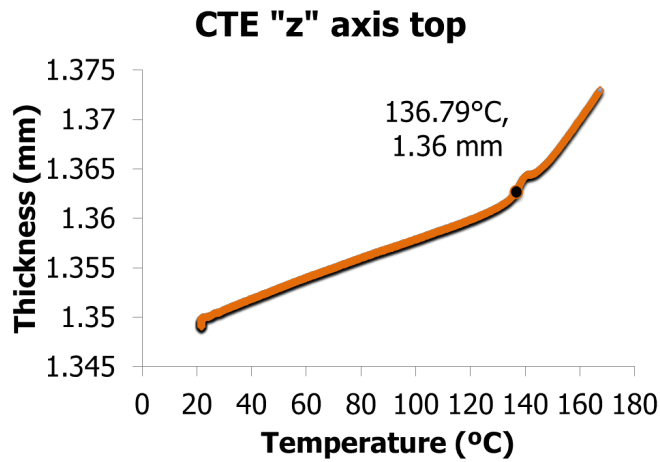


Figure 6.13: Coefficient of thermal expansion “z” axis at top area

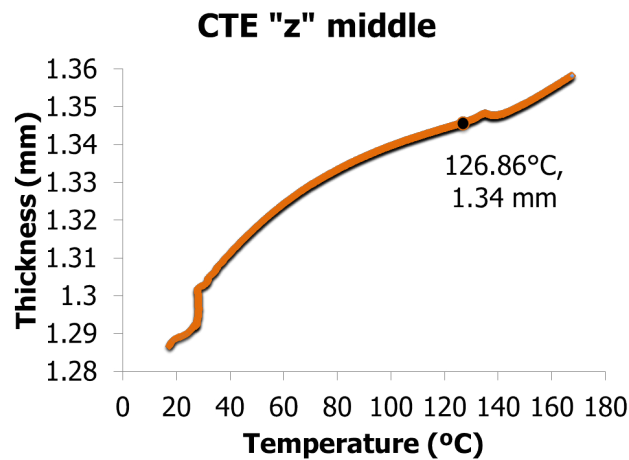


Figure 6.14: Coefficient of thermal expansion “z” axis at middle area

Figure 6.14 shows the results of the coefficient of thermal expansion in “z” axis at the middle area. The thermal expansion starts at 126.86°C as the black point marks, this type of performance is not typical for materials with these characteristics.

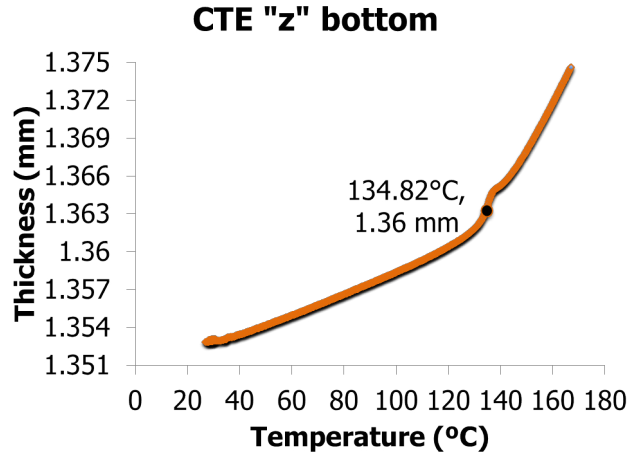


Figure 6.15: Coefficient of thermal expansion “z” axis at bottom area

Figure 6.15 represents the coefficient of thermal expansion at the bottom, the results are similar with the top area, the transition at the bottom occurs at 134.82°C, these values are similar to those reported in the literature so. Table 6.6 shows the thermal expansion coefficients before and after the glass transition temperature and thermal expansion percentages for “z” axis.

Table 6.6: Results at 3 areas for “z” axis

| Area | % thermal expansion | CTE before Tg | CTE after Tg |
|--------|---------------------|---------------|--------------|
| Top | 1,74 | 75.12 | 283.15 |
| Middle | 5.27 | 353.82 | 327.68 |
| Bottom | 1.58 | 61.19 | 285.14 |

CTE’s values for “z” axis are in a range of 50-70 ppm/°C before glass transition temperature [21], results at the middle area are 353.82 this value is higher, it is speculated that there is a concentration of heat, the heterogeneity in that area is predominant, copper, resin and glass fiber distribution is poor, generating thermal stresses and deformations along the axis, one of the reasons is that the resin expands with a higher rate of deformation in comparison with glass fiber.

Table 6.7 grouped the results of the coefficient of thermal expansion in “x”, “y” and “z” axis for the three areas.

Table 6.7: CTE results at 3 areas

| Area | Axis | CTE before tg | CTE after tg |
|--------|------|---------------|--------------|
| Top | “x” | 14.81 | 7.12 |
| | “y” | 13.29 | 1.53 |
| | “z” | 75.12 | 283.15 |
| Middle | “x” | 14.90 | 7.12 |
| | “y” | 13.08 | 2.11 |
| | “z” | 353.82 | 327.68 |
| Bottom | “x” | 15.30 | 9.00 |
| | “y” | 13.77 | 7.12 |
| | “z” | 61.19 | 285.14 |

Thermal expansion coefficient at “z” axis in middle area is not common according with supplier data sheet, results obtained were 353.82 ppm/°C before the glass transition temperature and 327.68 ppm/°C after the glass transition temperature. There is a considerable difference in material expansion, a possible heterogeneity between glass fiber and epoxy resin it can be speculated. The mismatch of thermal expansion coefficient at different PCB areas is a relevant factor generating deformations effect by heat loads, known as “warpage”.

6.4 Time to Delamination

Figure 6.16 is a thickness versus temperature chart of specimen took from the top area. Blue line corresponds the thickness and the red line the temperature, intentionally temperature above 260°C was raised in order to generate delaminations and explain it. Green box represents the constant temperature and bracket in black indicates a first elevation in thickness at 25 minutes. First peak represents a reversible deformation where the material expands and contracts, however, as the isotherm continues, peaks are generate, this means that the material is undergoing delamination and material suffers irreversible changes causing material disintegration.

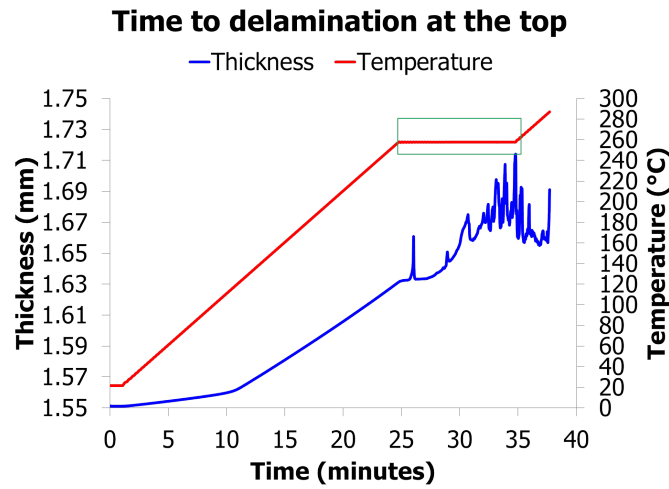


Figure 6.16: Time to delamination results at the top

Figure 6.17 and 6.18 shows the results obtained for specimens at middle and bottom area, respectively, both don't present changes in thickness during isothermal.

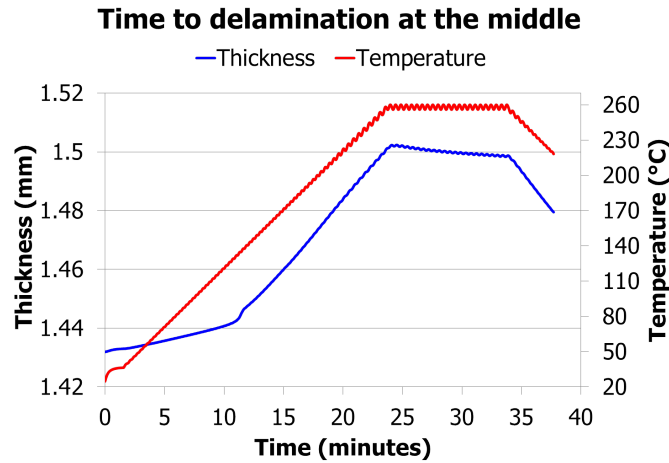


Figure 6.17: Time to delamination results at the middle

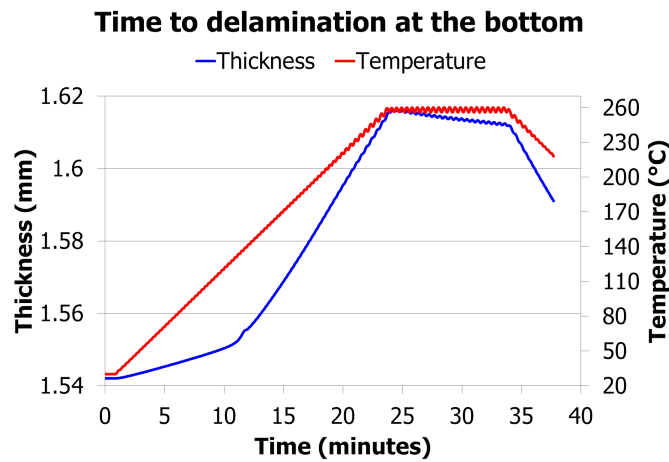


Figure 6.18: Time to delamination results at the bottom

The peak temperature during reflow process is 250°C, if the specimens stand the test during the isothermal at 260°C and there is not delamination, it is a guarantee that the material will not present delamination during reflow process, also the CTE mismatch in the material during the soldering cycles together with poor adhesive properties are the main reasons to delamination. This might occur in large solid Cu planes (bad adhesive) and blind vias (large CTE mismatch in “z” axis). Absorbed humidity causes high vapor pressure in the laminate, during the soldering process this may also contribute. Another problem is moisture trapped between the board layers occurring during PCB production. This will happened if moisture is not fully evaporated or if the material is not correctly cured during production. Large copper plane inside or on the board will raise the risk for delamination. The delaminations reduce board integrity and can permit moisture to pervade its structure [72].

Concluding specimens tested for time to delamination passed the test with no delaminations presented.

6.5 Water Absorption

Acceptable values is 0.15% according with material supplier date sheet. Table 6.8 shows the percentages obtained.

Table 6.8: Water absorption results

| Specimen | Mass before (gr) | Mass after (gr) | % absorption water |
|----------|------------------|-----------------|--------------------|
| 1 | 8.45 | 8.47 | 0.17 |
| 2 | 8.80 | 8.81 | 0.13 |
| 3 | 9.37 | 9.39 | 0.19 |
| 4 | 9.81 | 9.83 | 0.16 |

Specimens 1, 2 and 4 are slightly above with values of 0.17%, 0.13% and 0.16%, respectively, in the other hand specimen 3 with a value of % water absorption of 0.19%. This value is related with manufacturing laminated defects such as: incorrect resin/fiber impregnation, poor curing, existence of gaps, micro fractures, delaminations and weak fiberglass and epoxy resin interphase.

6.6 Bow and Twist Measurement

This section presents the “bow” and “twist” results as follows:

1. PCB “bow” after first reflow
2. PCB “bow” after second reflow
3. PCB “twist” after first reflow
4. PCB “twist” after second reflow

Initial data recorded are presented in appendix B.

6.6.1 PCB “bow” after first reflow

PCB’s were processed by the first reflow and data was recorded. Heights were recorded, designed by “R” at the four sides “AB”, “BC”, “CD” and “DA”. “R” is the distance between the surface and the PCB surface shown in figure 2.24.

Substituting values in equation 6.1 and taking “L” values from table B, “bow” after first reflow at each side were obtained the results are shown in figure 6.19. Data is presented in appendix C.1

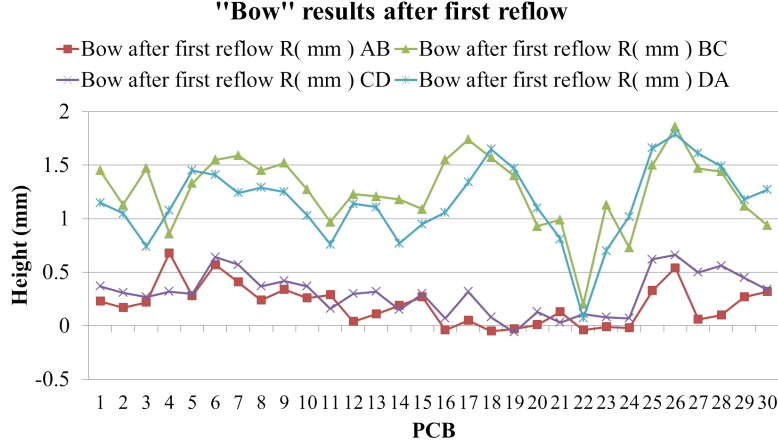


Figure 6.19: PCB “bow” results after first reflow

$$\%Bow = \frac{R}{L}(100) \quad (6.1)$$

According with figure 6.19 “BC” and “DA” sides presents higher elevations. “BC” side present a range of deformations from 0.2 mm (PCB #22) to 1.86 mm (PCB #26). PCB mean deformation in “BC” side is 1.26 mm. In the other hand “DA” side have a range of deformations from 0.07 mm (PCB #22) to 1.79 mm (PCB #26). PCB mean deformation in “DA” side is 1.15 mm.

Sides “AB” and “CD” presents less deformations as figure 6.19 shown, it is evident that the elevations are very similar for all PCB’s. “AB” side has a deformation range from -0.05 mm (PCB #18) to 0.68 mm (PCB #4), the mean deformation of “AB” side is 0.19 mm. For “CD” side the deformation range is from -0.06 mm to 0.66 mm and it’s mean deformation is 0.30 mm.

Concluding the sides susceptible to thermo-mechanical stresses are “BC” and “DA” sides causing higher values of “bow” after first reflow in comparison with “AB” and “CD” sides, which are more stable.

6.6.2 PCB “bow” after second reflow

Results of “bow” after second reflow was obtained as figure 6.20 shows. After second reflow PCB recovery it’s initial shape, sometimes this deformation goes to the op-

posite direction that's the reason of negative values, data are presented in appendix C.2. Now, as figure 6.20 shows.

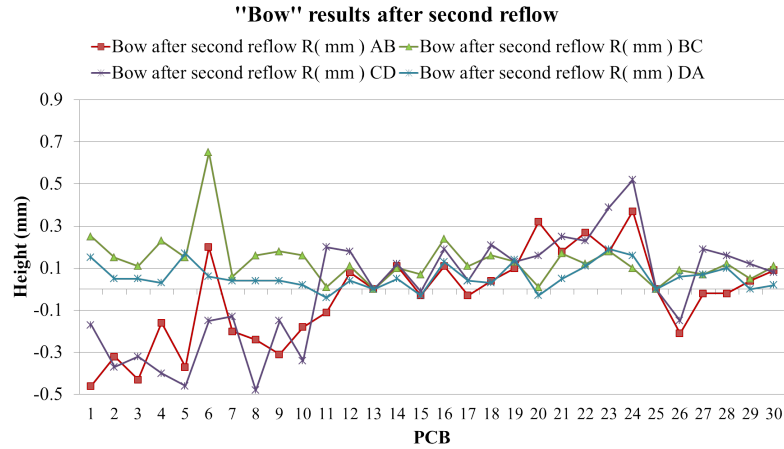


Figure 6.20: PCB “bow” results after second reflow

“BC” and “DA” sides are more stable, mostly of the PCB’s in those sides recovery almost it’s initial shape close to zero. “BC” side after second reflow present a range of deformation from 0.01 mm (PCB #11) to 0.65 mm (PCB #6) and it’s mean deformation is 0.14 mm; “DA” side has a range of deformation from -0.04 mm (PCB #11) to 0.19 mm (PCB #23) and it’s mean deformation is 0.06 mm.

Sides “AB” and “CD” presents after second reflow significant deformations, as figure 6.20 shows, it is evident that after second reflow process all the PCB’s deforms different, there is no relation between them, “AB” side presents a range of deformation from -0.46 mm (PCB # 1) to 0.37 mm (PCB #24), the mean deformation is -0.03 mm. For “CD” sides has a range of deformation from -0.48 mm (PCB #8) to 0.52 mm (PCB #24) with a mean deformation of 0.0014 mm.

After second reflow sides “AB” and “CD” deformations are unstable, apparently second reflow affects those sides, in the case of “BC” and “DA” sides, they return close to zero, recovering it’s initial shape, the major concerns after first and second reflow process are the “AB” and “CD” because mostly of the PCB are far from the zero or it’s original shape and can cause failures due to this deformations in subsequent processes.

6.6.3 PCB “twist” after first reflow

Results of “twist” after first reflow was obtained as figure 6.21 shows.

Data are presented in appendix D.1. Figure 6.21 shows a chart of corners height

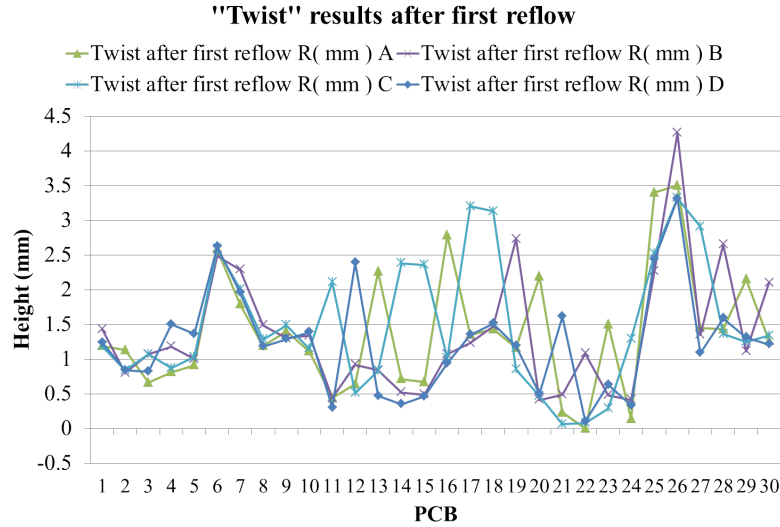


Figure 6.21: PCB “twist” results after first reflow

for each PCB. After first reflow process corner “A” deformations has a range from 0 mm (PCB #22) to 3.5 mm (PCB #26) with an average of 1.38 mm, corner “B” has varies from 0.41 mm (PCB #26) to 4.26 mm (PCB #26) and it’s average was 1.35 mm. In corner “C” the minimum value was 0.06 mm (PCB #21) and the maximum value was 3.32 mm (PCB #26) and it’s average is 1.49 mm. Corner “D” presented a range of deformations from 0.1 (PCB #22) mm to 3.31 mm (PCB #26) , the main deformation in corner “D” is 1.24 mm.

After first reflow process based on main deformation at each corner, the corners with higher deformation is corner “C”. Comparing the results, corner “A” and “B” deforms very similar. Corner “D” has the lowest value of corner deformation average, also it’s standard deviation is 0.73 mm, in contrast with the values o corners “A”, “B”, “C”, which are 0.86 mm, 0.86 mm and 0.92 mm, respectively.

6.6.4 PCB “twist” after second reflow

Data obtained for “twist” after second reflow is presented appendix D.2. Results of “twist” after second reflow was obtained as figure 6.22 shows.

After second reflow process corner “A” deformations has a range from -0.07 mm (PCB #18) to 3.4 mm (PCB #25) with an average of 0.42 mm, corner “B” has varies from -0.14 mm (PCB #6) to 2.27 mm (PCB #25) and it’s average was 0.34 mm. In corner “C” the minimum value was -0.1 mm (PCB #19) and the maximum value was 2.81 mm (PCB #22) and it’s average is 0.46 mm. Corner “D” presented a range of deformations from -0.06 (PCB #17) mm to 2.44 mm (PCB #25), the main

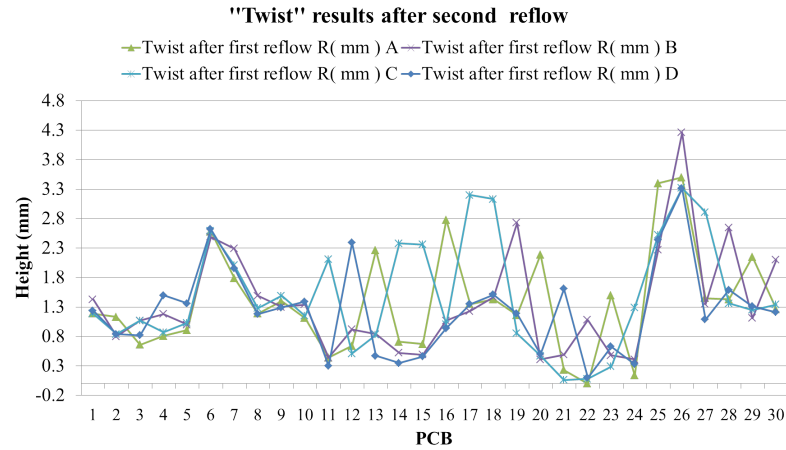


Figure 6.22: PCB “twist” results after second reflow

deformation in corner “D” is 0.36 mm.

After second reflow process based on main deformation at each corner, the corners with higher deformation is corner “C”. Comparing the results, corner “A” and “D” deforms very similar. Corner “B” and “D” has a similar corner deformation average. The lot with higher value of “bow” which is 0.56% means that presents 1.45 mm of height for “twist” it was obtained a 0.20% representing 3.06 mm of height.

6.7 Temperature Profile

Figure 6.23, 6.24, 6.25 and 6.26 represents data recorded of reflow oven obtained by four thermocouples, PCB was processed five times and a temperature vs time chart is obtained. There has been reported that temperature distributions during reflow ovens are not constant when a PCB is processed [49], [50]. Results obtained suggest that there is a difference in test 3 in comparison with the rest thermocouples, in test 1, 2, 4, and 5 profile temperature is very similar, concluding that the temperature distribution from the oven can be consider constant.

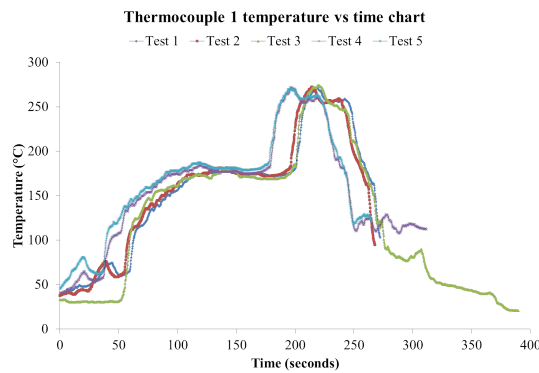


Figure 6.23: TC 1 temperature vs time

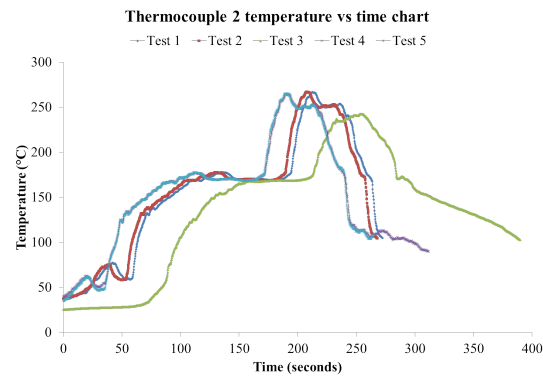


Figure 6.24: TC 2 temperature vs time

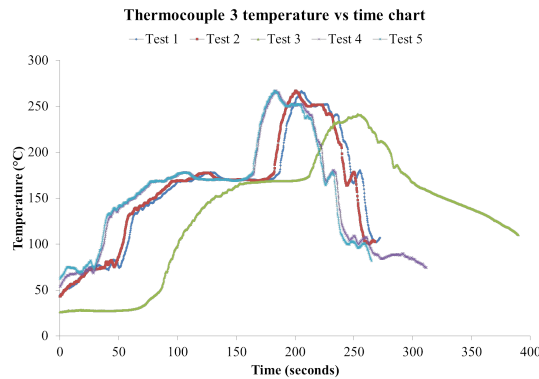


Figure 6.25: TC 3 temperature vs time

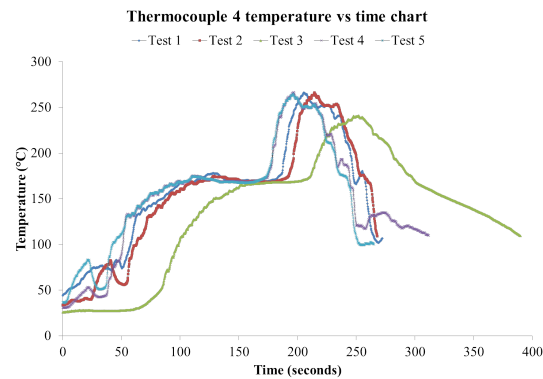


Figure 6.26: TC 4 temperature vs time

6.8 Summary of Results

Results obtained were analyzed and described in the previous sections. Thermal properties were determined, which are: glass transition temperature, decomposition temperature, coefficient of thermal expansion, time to delamination and % of water absorption, “bow” and “twist” data was generated after first and second reflow process, also a profile temperature was recorded in the reflow oven.

According with the thermal properties, the properties which do not correspond with the supplier values are: glass transition temperature, decomposition temperature, coefficient thermal expansion in “z” axis, whereas, absorption water and time to delamination pass the test performed. “Bow” and “twist” values exceeds the values establish on the standard [73] which are the 0.75% of it’s largest dimension. Profile temperature was determined by thermocouples, according with the data collected it is considered that the profile temperature has a slightly discrepancy in test 3 respect the rest of profiles.

The next section explain the conclusions and contributions of this research work, but before start the chapter, it is consider to gather a summary of the research work presented by one image shown in figure 6.27.

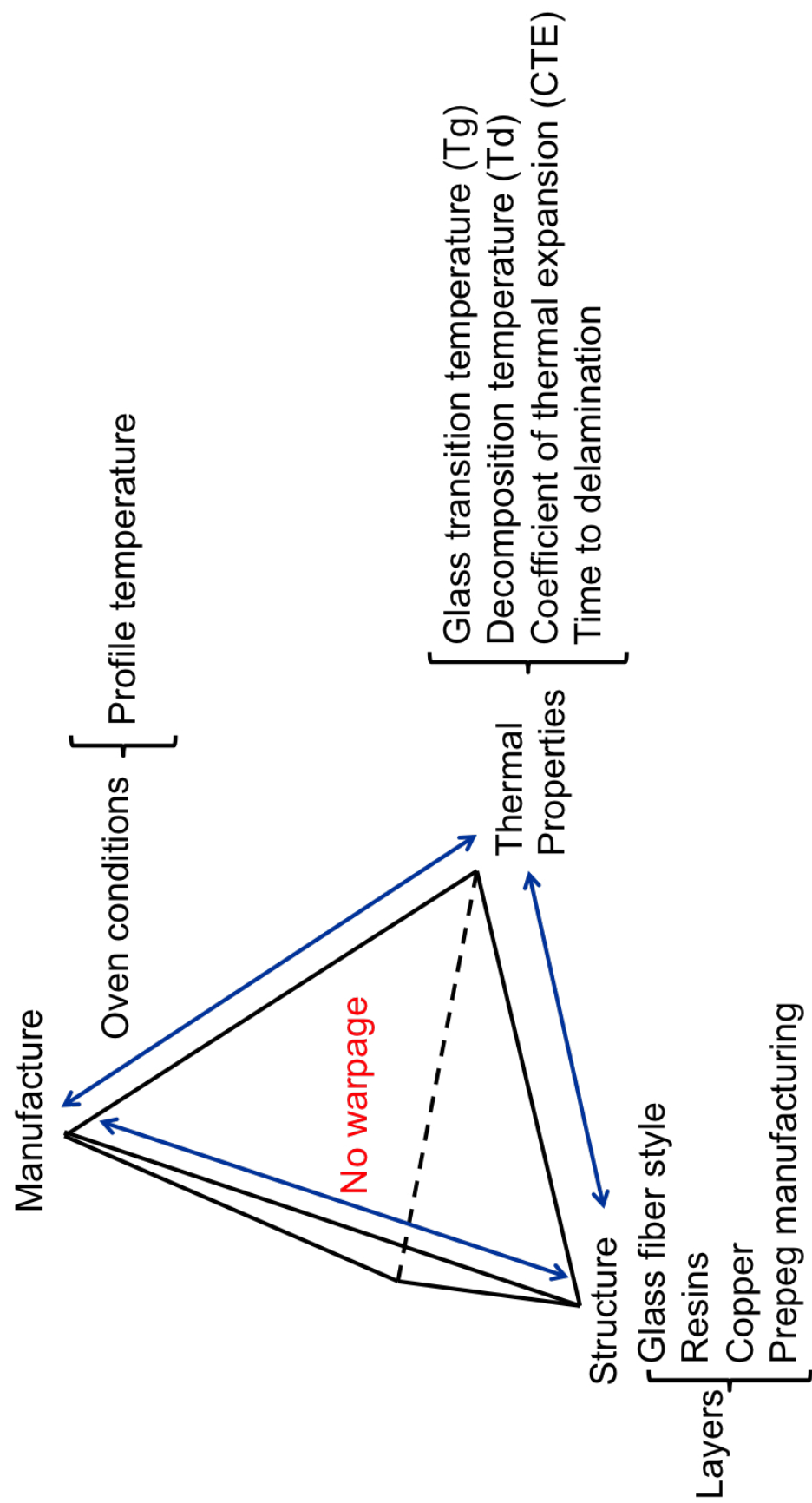


Figure 6.27: Material science tetrahedron

Figure 6.27 shows the scope of the research work, relating thermal properties, material structure and manufacture process, in this case, the reflow process. Figure 6.27 also is a representation of the contribution of this research work, there is no research work which gathered the different areas of PCB study, mostly of the researches focus only in thermal properties, reflow oven or simulations, but this a research work that contains a whole literature discussing the areas of interest for PCB's. Let's explain and detail what means each factor considered as warpage factor:

Structure

Structure means the characteristics of how the PCB is made, how many layers of glass fiber, resin and copper are present. This research work present clearly to the company, the different options of glass fiber that can be used according with:

- Chemical composition
- Glass fiber styles
- Glass fiber diameter

Literature consulted and provided allow a better understanding to PCB electrical engineer when designs the Printed Circuit Board, the glass fiber diameter is a complementary information, where it was demonstrated not in this research work but as a training course that diameters are different and how affect the stability of materials. Information about the reinforcement improvement was included, such as the addition of particles when the resin and glass fiber are fabricated, provides strength, decrease thermal loads, structure stability and the decrease of warpage. Another important constituent which was describe is the resins system, a whole information was consulted to evidence the different options of resins systems that can be used for PCBs since polyester resins to epoxy resins systems, which the latest is the resin system studied in this research work, also a general information about glass fiber styles was studied, some of them was described in Chapter 2, but in fact, there are many options and because of this research work engineers can selected or asked to the supplier the more convenient option depending of the PCB they are designing. Finally, the structure becomes complex when a lot of combination of glass fibers and resins systems are available to fabricate PCB's and this study contains a clearly information for consult this kind of information.

Thermal Properties

The figure 6.27 shows some of the thermal properties considered relevant to warpage phenomena, there are low, middle and high glass transition temperature resins systems, the elements at the end of the molecular chain is the factor which characterize what kind of glass transition it is. This knowledge is very useful because, engineers can gave an a idea just knowing the value of the Tg. Decomposition temperature is related with the glass transition temperature, but engineers has to pay attention in the decomposition temperature because is the temperature where the PCB starts a process of decomposition, so this study are capable to provides the methods and the knowledge to determined this property, also a typical range of decomposition temperatures are was presented in order to compare it with reflow process. A hole study of CTE was explained, defining CTE as one of the critical factors of warpage, it was demonstrated the difference according with the PCB area, state of the art literature was consulted showing different low CTEs but the cost of fabrication are higher that conventional materials used in Printed Circuit Boards, also the fabrication of PCB was investigated deeply and how the efficiency of this process affects PCB reliability. Time to delamination property provides the time when the PCB is exposed at high temperatures with no delaminations, the contribution was to presents the information clearly and explained the test to know the time to delamination depending of the resin system.

Oven Conditions

The reflow oven is the latest factors that was studied, it was found a complete kind of literature of reflow ovens. Contribution about reflow ovens was to explain the factors that affects warpage, such as: non uniform temperature distributions, mismatch of convection thermal coefficients between stages, a thermal shock due to the sudden cooling after reflow process. Based on researches investigated it was suggested to performed a slower cooling rate to allow the material recovery after temperature exposures, ovens with additional cooling stages. The oven studied in this research work as it shown in previous chapters has only two stages of cooling and the temperature change between stage seven and eight is drastic.

This factors are the responsible which cause warpage, the contribution of this research work is to involve all of them as entire study due to there is no literature that that take in consideration together. A wide options can be suggest to improve each factor individually to get a common objeive: no warpage.

Chapter 7

Conclusions and Contributions

7.1 Conclusions

PCB thermo-mechanical performance depends of material thermal properties and reflow process conditions. Thermal properties are governed by the constituents materials such as: epoxy resin tg, glass fiber stack up, % of copper. In the other hand based on the reflow oven analysis, an homogenous heat transfer allow a better distribution trough PCB during reflow process. In the material studied:

- Glass transition temperature average was 138°C.
- Decomposition temperature average was 300°C.
- Coefficient of thermal expansion in 3 axis (“x”, “y” and “z”) were determined at three different locations, top, middle and bottom.

“x” axis CTE below and after Tg are similar at the three areas, 15 ppm/°C and 7.67 ppm/°C, respectively.

“y” axis CTE after Tg at the bottom differs considerably in comparison with top and middle areas, 7.11 ppm/°C at the bottom and 2.11 ppm/°C for top and middle areas, that means material expands at different rate at the middle area along “y” axis.

“z” axis CTE before and after Tg at the middle is higher than top and bottom areas, normal values are in a range 60-75 ppm/°C before Tg and 280-300 ppm/°C after Tg. Results obtained at the middle area for “z” axis are 354.59 ppm/°C before Tg and 312.11 ppm/°C, this result is the most critical factor for warpage, because when a thermal load is applied, the material starts the expansion in “z” axis at the middle area, whereas the top and bottom

areas needs expands slowly and with lowest values, this difference generates mismatch coefficients and as a consequence thermal stresses represented as mechanical distortions

- Time to delamination test was performed and materials used for PCB's are capable to be exposed at 260°C during reflow process with no presence of delaminations by the influence of thermal stresses at glass fiber and resin interphases.
- Absorption water measurements results was obtained and materiales accomplished standard values, which has a limit of percentage of absorption of 0.15%.

All the thermal properties corresponds with data sheet materials provided by PCB supplier, except the CTE after Tg at the bottom in “y” axis, also in “z” axis at the middle values are higher before and after Tg. “Bow” and “twist” conclusions:

- After first reflow “BC” and “DA” sides has higher values of “bow”; “AB” and “CD” sides are more stable, but after second reflow “AB” and “CD” sides are unstable, “BC” and “DA” sides return close to zero, recovering it's initial shape. The major concerns after first and second reflow process are the “AB” and “CD” they are far from it's original shape.
- Corner “C” has higher deformation after first and second reflow process. Corners “A” and “B” deforms very similar during reflow process, corner “D” has the lowest value of deformation. After second reflow process corners “A”, “B” and “D” deforms very similar.

Reflow oven studied:

- Reflow oven presents a constant temperature distributions across stages each time when PCB is processed.
- Heat transfer trough PCB is slightly different at PCB areas, this changes are not relevant for warpage generation.

CTE differences is one of the key factor which generates non uniform material expansions trough the PCB, these differences origins that the PCB deforms differently at different areas, causing “bow” and “twist”.

7.2 Contributions

The main contribution of this research work is to relate the structure, process and material thermal properties determining warpage by thermo-mechanical study, also this work consider real products of the company to obtain statistical data about PCB distortions and predict preferential areas of “warpage”.

The present work provides a whole study of material thermal properties, reflow conditions and bow/twist, which are the key factors of “warpage”. The information generated is useful to establish a preliminary projection of the PCB thermo-mechanical performance based on the thermal properties and the deformations data collected during reflow process. This research work considered different PCB areas of study, it is found that there are a mismatch between them, it is speculated a relationship with preferential deformations during reflow process.

- This is the first research work focused in PCB thermo mechanical performance during reflow process at Yazaki Monterrey. Generating knowledge about the key factors of “warpage” during reflow process. The information developed allows a guideline for engineers to design and process PCB’s.
- “bow” and “twist” data of materiales used for PCB’s are illustrated, a instructional manual was developed to obtain “bow” and “twist” measurements it can be use for internal process.
- This is the first research work which gathered material properties, PCB deformations and reflow ovens conditions in order to get a better understand about thermo-mechanical performance.
- Research work suggests:

Material properties and characteristics must be requested to supplier, it must contain: epoxy resin system, glass fiber style, stack up, a thermal characterization details which contains the principal thermal properties: glass transition temperature, decomposition temperature, coefficient of thermal expansion, time to delamination, absorption water.

Performed a PCB characterization to corroborate supplier information. Thermal tests and “bow” and “twist” measurements must be made.

PCB thermal performance simulation is suggested as a complementary factor in order to predict PCB thermo-mechanical performance during reflow process.

Appendix A

Heat Transfer for Base Materials

Base materials heat transfer were obtained considering materials as layers obtaining the values individually, conduction is the heat transfer mechanism considered, which formula is:

$$q = \frac{kA\delta T}{s} \quad (A.1)$$

TableA.1 shows the results summarized

| <i>Material</i> | <i>q(kW)</i> | <i>k(W/m · °C)</i> | <i>Area(m²)</i> | <i>δT(°C)</i> | <i>s(m)</i> |
|-----------------|--------------|--------------------|----------------------------|---------------|-----------------------|
| <i>Copper</i> | 185,605.7 | 401 | 0.072 | 225 | 3.5×10^{-5} |
| <i>Epoxy</i> | 52 | 0.35 | 0.072 | 225 | 1.09×10^{-4} |
| <i>Glass</i> | 6.9 | 0.04 | 0.072 | 225 | 9.4×10^{-5} |

Table A.1: Heat transfer of base materials

$$q_{copper} = \frac{401(\frac{W}{m \cdot ^\circ C})(0.072m^2)(225^\circ C)}{3.5 \times 10^{-5}m} = 185,695.7kW \quad (A.2)$$

$$q_{epoxy} = \frac{0.35(\frac{W}{m \cdot ^\circ C})(0.072m^2)(225^\circ C)}{1.09 \times 10^{-4}m} = 52kW \quad (A.3)$$

$$q_{glass} = \frac{0.04(\frac{W}{m \cdot ^\circ C})(0.072m^2)(225^\circ C)}{9.4 \times 10^{-5}m} = 6.9kW \quad (A.4)$$

Appendix B

PCB's dimensions

| <i>PCB</i> | <i>Thickness(mm)</i> | | | | <i>Diagonals(mm)</i> | | <i>Dimensions</i> | | | |
|------------|----------------------|----------|----------|----------|----------------------|-----------|-------------------|-----------|-----------|-----------|
| | <i>A</i> | <i>B</i> | <i>C</i> | <i>D</i> | <i>AC</i> | <i>BD</i> | <i>AB</i> | <i>BC</i> | <i>CD</i> | <i>DA</i> |
| 1 | 1.58 | 1.56 | 1.57 | 1.58 | 378.01 | 378.12 | 290.03 | 245.09 | 290.10 | 245.08 |
| 2 | 1.57 | 1.58 | 1.58 | 1.57 | 378.04 | 378.11 | 290.04 | 245.10 | 290.10 | 245.08 |
| 3 | 1.59 | 1.49 | 1.48 | 1.57 | 378.03 | 378.09 | 290.07 | 245.10 | 290.11 | 245.11 |
| 4 | 1.5 | 1.55 | 1.58 | 1.49 | 378.04 | 378.06 | 290.04 | 245.12 | 290.07 | 245.09 |
| 5 | 1.6 | 1.56 | 1.59 | 1.5 | 378.04 | 378.07 | 290.09 | 245.20 | 290.11 | 245.10 |
| 6 | 1.57 | 1.55 | 1.56 | 1.58 | 378.02 | 378.07 | 290.05 | 245.10 | 290.10 | 245.07 |
| 7 | 1.54 | 1.57 | 1.57 | 1.53 | 377.97 | 378.06 | 289.95 | 245.10 | 290.09 | 245.08 |
| 8 | 1.54 | 1.57 | 1.58 | 1.57 | 378.00 | 378.07 | 290.01 | 245.08 | 290.10 | 245.03 |
| 9 | 1.54 | 1.58 | 1.58 | 1.57 | 378.08 | 378.02 | 290.08 | 245.09 | 290.11 | 245.07 |
| 10 | 1.57 | 1.59 | 1.58 | 1.58 | 378.02 | 378.09 | 290.03 | 245.13 | 290.16 | 245.11 |
| 11 | 1.66 | 1.60 | 1.65 | 1.62 | 378.0 | 378.05 | 290.01 | 245.11 | 290.10 | 245.05 |
| 12 | 1.64 | 1.53 | 1.50 | 1.56 | 378.02 | 378.05 | 290.07 | 245.11 | 290.05 | 245.05 |
| 13 | 1.63 | 1.57 | 1.58 | 1.55 | 378.03 | 378.06 | 290.05 | 245.06 | 290.11 | 245.02 |
| 14 | 1.63 | 1.57 | 1.58 | 1.56 | 378.00 | 378.08 | 290.09 | 245.09 | 290.13 | 245.05 |
| 15 | 1.63 | 1.58 | 1.61 | 1.61 | 378.01 | 378.09 | 290.05 | 245.14 | 290.15 | 245.07 |
| 16 | 1.64 | 1.56 | 1.59 | 1.62 | 378.03 | 378.06 | 290.04 | 245.06 | 290.10 | 245.04 |
| 17 | 1.68 | 1.63 | 1.56 | 1.64 | 378.03 | 378.10 | 290.09 | 245.08 | 290.14 | 245.10 |
| 18 | 1.66 | 1.63 | 1.57 | 1.70 | 378.02 | 378.05 | 290.05 | 245.10 | 290.11 | 245.09 |
| 19 | 1.65 | 1.64 | 1.70 | 1.61 | 378.03 | 378.06 | 290.06 | 245.09 | 290.08 | 245.05 |
| 20 | 1.70 | 1.64 | 1.65 | 1.62 | 378.04 | 378.07 | 290.06 | 245.08 | 290.11 | 245.05 |
| 21 | 1.54 | 1.58 | 1.64 | 1.56 | 378.04 | 378.09 | 289.98 | 245.08 | 290.12 | 245.03 |
| 22 | 1.65 | 1.64 | 1.59 | 1.65 | 378.05 | 378.11 | 290.10 | 245.14 | 290.09 | 245.05 |
| 23 | 1.62 | 1.58 | 1.58 | 1.50 | 378.07 | 378.10 | 290.09 | 245.11 | 290.10 | 245.10 |
| 24 | 1.62 | 1.57 | 1.55 | 1.58 | 378.02 | 378.13 | 290.08 | 245.12 | 290.18 | 245.08 |
| 25 | 1.60 | 1.51 | 1.50 | 1.57 | 378.03 | 378.06 | 290.02 | 245.10 | 290.10 | 245.05 |
| 26 | 1.65 | 1.54 | 1.58 | 1.55 | 378.02 | 378.08 | 290.01 | 245.04 | 290.03 | 245.06 |
| 27 | 1.64 | 1.55 | 1.55 | 1.56 | 378.02 | 378.07 | 290.05 | 245.10 | 290.05 | 245.04 |
| 28 | 1.65 | 1.56 | 1.53 | 1.52 | 378.01 | 378.06 | 290.08 | 245.11 | 290.07 | 245.06 |
| 29 | 1.57 | 1.60 | 1.57 | 1.60 | 378.02 | 378.10 | 290.10 | 245.09 | 290.09 | 245.03 |
| 30 | 1.56 | 1.66 | 1.59 | 1.60 | 378.03 | 378.08 | 290.12 | 245.06 | 290.05 | 245.09 |

Table B.1: PCB's dimensions

Appendix C

Bow Results

C.1 Bow results after first reflow

| <i>PCB</i> | <i>Height(mm)</i> | | | | <i>%bow</i> | | | |
|------------|-------------------|----------------|----------------|----------------|-------------|-----------|-----------|-----------|
| | <i>R(mm)AB</i> | <i>R(mm)BC</i> | <i>R(mm)CD</i> | <i>R(mm)DA</i> | <i>AB</i> | <i>BC</i> | <i>CD</i> | <i>DA</i> |
| 1 | 0.23 | 1.45 | 0.37 | 1.15 | 0.08 | 0.59 | 0.13 | 0.47 |
| 2 | 0.17 | 1.13 | 0.31 | 1.05 | 0.06 | 0.46 | 0.11 | 0.43 |
| 3 | 0.22 | 1.47 | 0.27 | 0.74 | 0.08 | 0.60 | 0.09 | 0.30 |
| 4 | 0.68 | 0.86 | 0.32 | 1.08 | 0.23 | 0.35 | 0.11 | 0.44 |
| 5 | 0.28 | 1.33 | 0.30 | 1.45 | 0.10 | 0.54 | 0.10 | 0.59 |
| 6 | 0.57 | 1.55 | 0.64 | 1.41 | 0.20 | 0.63 | 0.22 | 0.58 |
| 7 | 0.41 | 1.59 | 0.57 | 1.24 | 0.14 | 0.65 | 0.20 | 0.51 |
| 8 | 0.24 | 1.45 | 0.37 | 1.29 | 0.08 | 0.59 | 0.13 | 0.53 |
| 9 | 0.34 | 1.52 | 0.42 | 1.25 | 0.12 | 0.62 | 0.14 | 0.51 |
| 10 | 0.26 | 1.27 | 0.37 | 1.03 | 0.09 | 0.52 | 0.13 | 0.42 |
| 11 | 0.29 | 0.97 | 0.16 | 0.76 | 0.10 | 0.40 | 0.06 | 0.31 |
| 12 | 0.04 | 1.23 | 0.30 | 1.14 | 0.01 | 0.50 | 0.10 | 0.47 |
| 13 | 0.11 | 1.21 | 0.32 | 1.11 | 0.04 | 0.49 | 0.11 | 0.45 |
| 14 | 0.19 | 1.18 | 0.15 | 0.77 | 0.07 | 0.48 | 0.05 | 0.31 |
| 15 | 0.27 | 1.09 | 0.30 | 0.95 | 0.09 | 0.44 | 0.10 | 0.39 |
| 16 | -0.04 | 1.55 | 0.07 | 1.06 | -0.01 | 0.63 | 0.02 | 0.43 |
| 17 | 0.05 | 1.74 | 0.32 | 1.34 | 0.02 | 0.71 | 0.11 | 0.55 |
| 18 | -0.05 | 1.57 | 0.08 | 1.65 | -0.02 | 0.64 | 0.03 | 0.67 |
| 19 | -0.03 | 1.40 | -0.06 | 1.47 | -0.01 | 0.57 | -0.02 | 0.60 |
| 20 | 0.01 | 0.93 | 0.13 | 1.10 | 0.00 | 0.38 | 0.04 | 0.45 |
| 21 | 0.13 | 0.99 | 0.03 | 0.81 | 0.04 | 0.01 | 0.40 | 0.33 |
| 22 | -0.04 | 0.20 | 0.11 | 0.07 | -0.01 | 0.04 | 0.08 | 0.03 |
| 23 | -0.01 | 1.13 | 0.08 | 0.70 | 0.00 | 0.03 | 0.46 | 0.29 |
| 24 | -0.02 | 0.73 | 0.07 | 1.02 | -0.01 | 0.02 | 0.30 | 0.42 |
| 25 | 0.33 | 1.50 | 0.62 | 1.66 | 0.11 | 0.21 | 0.61 | 0.68 |
| 26 | 0.54 | 1.86 | 0.66 | 1.79 | 0.19 | 0.23 | 0.76 | 0.73 |
| 27 | 0.06 | 1.47 | 0.50 | 1.61 | 0.02 | 0.17 | 0.60 | 0.66 |
| 28 | 0.10 | 1.44 | 0.56 | 1.49 | 0.03 | 0.19 | 0.59 | 0.61 |
| 29 | 0.27 | 1.12 | 0.45 | 1.18 | 0.09 | 0.16 | 0.46 | 0.48 |
| 30 | 0.32 | 0.94 | 0.34 | 1.27 | 0.11 | 0.12 | 0.38 | 0.52 |

Table C.1: PCB bow results after first reflow

C.2 Bow results after second reflow

| <i>PCB</i> | <i>Height(mm)</i> | | | | <i>%bow</i> | | | |
|------------|-------------------|----------------|----------------|----------------|-------------|-----------|-----------|-----------|
| | <i>R(mm)AB</i> | <i>R(mm)BC</i> | <i>R(mm)CD</i> | <i>R(mm)DA</i> | <i>AB</i> | <i>BC</i> | <i>CD</i> | <i>DA</i> |
| 1 | -0.46 | 0.25 | -0.17 | 0.15 | -0.16 | 0.10 | -0.06 | 0.06 |
| 2 | -0.32 | 0.15 | -0.37 | 0.05 | -0.11 | 0.06 | -0.13 | 0.02 |
| 3 | -0.43 | 0.11 | -0.32 | 0.05 | -0.15 | 0.04 | -0.11 | 0.02 |
| 4 | -0.16 | 0.23 | -0.40 | 0.03 | -0.06 | 0.09 | -0.14 | 0.01 |
| 5 | -0.37 | 0.15 | -0.46 | 0.17 | -0.13 | 0.06 | -0.16 | 0.07 |
| 6 | 0.20 | 0.65 | -0.15 | 0.06 | 0.07 | 0.27 | -0.05 | 0.02 |
| 7 | -0.20 | 0.06 | -0.13 | 0.04 | -0.07 | 0.02 | -0.04 | 0.02 |
| 8 | -0.24 | 0.16 | -0.48 | 0.04 | -0.08 | 0.07 | -0.17 | 0.02 |
| 9 | -0.31 | 0.18 | -0.15 | 0.04 | -0.11 | 0.07 | -0.05 | 0.02 |
| 10 | -0.18 | 0.16 | -0.34 | 0.02 | -0.06 | 0.07 | -0.12 | 0.01 |
| 11 | -0.11 | 0.01 | 0.20 | -0.04 | -0.04 | 0.00 | 0.07 | -0.02 |
| 12 | 0.08 | 0.11 | 0.18 | 0.04 | 0.03 | 0.04 | 0.06 | 0.02 |
| 13 | -1.63 | -1.57 | -1.58 | -1.55 | -0.56 | -0.64 | -0.54 | -0.63 |
| 14 | 0.11 | 0.10 | 0.12 | 0.05 | 0.04 | 0.04 | 0.04 | 0.02 |
| 15 | -0.03 | 0.07 | -0.01 | -0.03 | -0.01 | 0.03 | 0.00 | -0.01 |
| 16 | 0.11 | 0.24 | 0.19 | 0.13 | 0.04 | 0.10 | 0.07 | 0.05 |
| 17 | -0.03 | 0.11 | 0.04 | 0.04 | -0.01 | 0.04 | 0.01 | 0.02 |
| 18 | 0.04 | 0.16 | 0.21 | 0.03 | 0.01 | 0.07 | 0.07 | 0.01 |
| 19 | 0.10 | 0.13 | 0.13 | 0.14 | 0.03 | 0.05 | 0.04 | 0.06 |
| 20 | 0.32 | 0.01 | 0.16 | -0.03 | 0.11 | 0.00 | 0.06 | -0.01 |
| 21 | 0.18 | 0.17 | 0.25 | 0.05 | 0.06 | 0.05 | 0.09 | 0.02 |
| 22 | 0.27 | 0.12 | 0.23 | 0.11 | 0.09 | 0.05 | 0.08 | 0.04 |
| 23 | 0.18 | 0.18 | 0.39 | 0.19 | 0.06 | 0.07 | 0.13 | 0.08 |
| 24 | 0.37 | 0.10 | 0.52 | 0.16 | 0.13 | 0.04 | 0.18 | 0.07 |
| 25 | -1.60 | -1.51 | -1.50 | -1.57 | -0.55 | -0.62 | -0.52 | -0.64 |
| 26 | -0.21 | 0.09 | -0.15 | 0.06 | -0.07 | 0.04 | -0.05 | 0.02 |
| 27 | -0.02 | 0.07 | 0.19 | 0.07 | -0.01 | 0.03 | 0.07 | 0.03 |
| 28 | -0.02 | 0.12 | 0.16 | 0.10 | -0.01 | 0.05 | 0.06 | 0.04 |
| 29 | 0.04 | 0.05 | 0.12 | 0.00 | 0.01 | 0.02 | 0.04 | 0.00 |
| 30 | 0.09 | 0.11 | 0.08 | 0.02 | 0.03 | 0.04 | 0.03 | 0.01 |

Table C.2: PCB bow results after second reflow

Appendix D

Twist Results

D.1 Twist results after first reflow

| <i>PCB</i> | <i>CornerHeightR(mm)</i> | | | | <i>%twist</i> | | | |
|------------|--------------------------|---------------|---------------|---------------|---------------|----------|----------|----------|
| | <i>R(mm)A</i> | <i>R(mm)B</i> | <i>R(mm)C</i> | <i>R(mm)D</i> | <i>A</i> | <i>B</i> | <i>C</i> | <i>D</i> |
| 1 | 1.19 | 1.43 | 1.19 | 1.24 | 0.16 | 0.19 | 0.16 | 0.16 |
| 2 | 1.13 | 0.80 | 0.84 | 0.84 | 0.15 | 0.11 | 0.11 | 0.11 |
| 3 | 0.66 | 1.07 | 1.07 | 0.82 | 0.09 | 0.14 | 0.14 | 0.11 |
| 4 | 0.81 | 1.18 | 0.87 | 1.50 | 0.11 | 0.16 | 0.12 | 0.20 |
| 5 | 1.91 | 1.00 | 1.03 | 1.36 | 0.12 | 0.13 | 0.14 | 0.18 |
| 6 | 2.58 | 2.49 | 2.59 | 2.62 | 0.34 | 0.33 | 0.34 | 0.35 |
| 7 | 1.79 | 2.29 | 2.01 | 1.96 | 0.24 | 0.30 | 0.27 | 0.26 |
| 8 | 1.19 | 1.49 | 1.28 | 1.18 | 0.16 | 0.20 | 0.17 | 0.16 |
| 9 | 1.40 | 1.30 | 1.49 | 1.29 | 0.19 | 0.17 | 0.20 | 0.17 |
| 10 | 1.11 | 1.34 | 1.15 | 1.39 | 0.15 | 0.18 | 0.15 | 0.18 |
| 11 | 0.44 | 0.44 | 2.11 | 0.30 | 0.06 | 0.06 | 0.28 | 0.04 |
| 12 | 0.64 | 0.92 | 0.51 | 2.39 | 0.08 | 0.12 | 0.07 | 0.32 |
| 13 | 2.26 | 0.84 | 0.83 | 0.47 | 0.30 | 0.11 | 0.11 | 0.06 |
| 14 | 0.71 | 0.52 | 2.38 | 0.35 | 0.09 | 0.07 | 0.31 | 0.05 |
| 15 | 0.67 | 0.49 | 2.36 | 0.46 | 0.09 | 0.06 | 0.31 | 0.06 |
| 16 | 2.78 | 1.07 | 1.01 | 0.94 | 0.37 | 0.14 | 0.13 | 0.12 |
| 17 | 1.35 | 1.23 | 3.20 | 1.35 | 0.18 | 0.16 | 0.42 | 0.18 |
| 18 | 1.43 | 1.47 | 3.13 | 1.51 | 0.19 | 0.19 | 0.41 | 0.20 |
| 19 | 1.16 | 2.73 | 0.85 | 1.19 | 0.15 | 0.36 | 0.11 | 0.16 |
| 20 | 2.19 | 0.41 | 0.47 | 0.50 | 0.29 | 0.05 | 0.06 | 0.07 |
| 21 | 0.23 | 0.49 | 0.06 | 1.61 | 0.03 | 0.06 | 0.01 | 0.21 |
| 22 | 0.00 | 1.08 | 0.08 | 0.10 | 0.00 | 0.14 | 0.01 | 0.01 |
| 23 | 1.50 | 0.48 | 0.29 | 0.63 | 0.20 | 0.06 | 0.04 | 0.08 |
| 24 | 0.14 | 0.41 | 1.29 | 0.33 | 0.02 | 0.05 | 0.17 | 0.04 |
| 25 | 3.40 | 2.27 | 2.52 | 2.44 | 0.45 | 0.30 | 0.33 | 0.32 |
| 26 | 3.50 | 4.26 | 3.32 | 3.31 | 0.46 | 0.56 | 0.44 | 0.44 |
| 27 | 1.45 | 1.35 | 2.91 | 1.09 | 0.19 | 0.18 | 0.38 | 0.14 |
| 28 | 1.43 | 2.65 | 1.36 | 1.59 | 0.19 | 0.35 | 0.18 | 0.21 |
| 29 | 2.15 | 1.11 | 1.25 | 1.31 | 0.28 | 0.15 | 0.17 | 0.17 |
| 30 | 1.26 | 2.10 | 1.34 | 1.21 | 0.17 | 0.28 | 0.18 | 0.16 |

Table D.1: PCB twist results after first reflow

D.2 Twist results after second reflow

| PCB | CornerHeightR(mm) | | | | %twist | | | |
|-----|-------------------|--------|--------|--------|--------|-------|-------|-------|
| | R(mm)A | R(mm)B | R(mm)C | R(mm)D | A | B | C | D |
| 1 | -0.04 | 0.16 | 0.22 | 0.24 | -0.01 | 0.02 | 0.03 | 0.03 |
| 2 | 0.14 | 0.20 | 0.19 | 0.33 | 0.02 | 0.03 | 0.03 | 0.04 |
| 3 | 0.21 | 0.02 | 0.14 | 0.24 | 0.03 | 0.00 | 0.02 | 0.03 |
| 4 | 0.04 | 0.29 | 0.14 | 0.18 | 0.01 | 0.04 | 0.02 | 0.02 |
| 5 | -0.06 | 0.27 | 0.05 | 0.20 | -0.01 | 0.04 | 0.01 | 0.03 |
| 6 | -0.02 | -0.14 | 0.00 | 0.20 | 0.00 | -0.02 | 0.00 | 0.03 |
| 7 | 0.07 | 0.06 | 0.04 | 0.18 | 0.01 | 0.01 | 0.01 | 0.02 |
| 8 | 0.26 | 0.26 | 0.03 | 0.13 | 0.03 | 0.03 | 0.00 | 0.02 |
| 9 | 0.06 | 0.22 | 0.03 | 0.00 | 0.01 | 0.03 | 0.00 | 0.00 |
| 10 | 0.14 | 0.31 | 0.02 | 0.14 | 0.02 | 0.04 | 0.00 | 0.02 |
| 11 | 0.78 | 0.23 | 0.32 | 0.25 | 0.10 | 0.03 | 0.04 | 0.03 |
| 12 | 0.56 | 0.17 | 0.33 | 0.19 | 0.07 | 0.02 | 0.04 | 0.03 |
| 13 | -1.63 | -1.57 | -1.58 | -1.55 | -0.22 | -0.21 | -0.21 | -0.20 |
| 14 | 0.73 | 0.25 | 0.09 | 0.26 | 0.10 | 0.03 | 0.01 | 0.03 |
| 15 | 0.21 | 0.25 | 0.65 | 0.23 | 0.03 | 0.03 | 0.09 | 0.03 |
| 16 | 0.42 | 0.02 | 0.04 | 0.11 | 0.06 | 0.00 | 0.01 | 0.01 |
| 17 | -0.02 | -0.03 | 0.03 | -0.06 | 0.00 | 0.00 | 0.00 | -0.01 |
| 18 | -0.07 | -0.02 | 0.06 | 0.43 | -0.01 | 0.00 | 0.01 | 0.06 |
| 19 | -0.01 | 0.03 | -0.10 | 0.45 | 0.00 | 0.00 | -0.01 | 0.06 |
| 20 | 0.02 | 0.08 | 0.62 | 0.02 | 0.00 | 0.01 | 0.08 | 0.00 |
| 21 | 0.52 | 0.52 | 1.82 | 0.08 | 0.07 | 0.07 | 0.24 | 0.01 |
| 22 | 1.52 | 1.68 | 2.81 | 1.52 | 0.20 | 0.22 | 0.37 | 0.20 |
| 23 | 0.54 | 0.96 | 1.92 | 0.14 | 0.07 | 0.13 | 0.25 | 0.02 |
| 24 | 0.47 | 0.28 | 0.15 | 1.25 | 0.06 | 0.04 | 0.02 | 0.17 |
| 25 | -1.60 | -1.51 | -1.50 | -1.57 | -0.21 | -0.20 | -0.20 | -0.21 |
| 26 | -0.06 | 0.23 | -0.03 | 0.03 | -0.01 | 0.03 | 0.00 | 0.00 |
| 27 | 0.20 | 0.10 | 0.02 | 0.89 | 0.03 | 0.01 | 0.00 | 0.12 |
| 28 | 0.10 | 0.54 | 0.20 | 0.12 | 0.01 | 0.07 | 0.03 | 0.02 |
| 29 | 0.20 | 0.27 | 0.83 | 0.10 | 0.03 | 0.04 | 0.11 | 0.01 |
| 30 | 0.30 | 0.02 | 0.01 | 0.18 | 0.04 | 0.00 | 0.00 | 0.02 |

Table D.2: PCB twist results after second reflow

Bibliography

- [1] Kris Vasoya Alex Mangroli. Optimizing thermal and mechanical performance in pcbs. *Global SMT and Packaging*, pages 10–12, December 2007.
- [2] Charles A. Harper. *Electronics Materials and Processes Handbook*. Mc-Graw-Hill, 2003.
- [3] Jr. Clyde F. Coombs. *Printed Circuits Handbook*. Mc-Graw-Hill, 6 edition, 2008.
- [4] Anthony V. Longobardo. *Glass Fibers for Printed Circuit Boards*. F.T. Wallenberger, P.A. Bingham. Springer Science + Business Media, LLC, 2010.
- [5] Chandru Idnani. Impact of new materials and processes on manufacturing: Green (pb and halide free), rohs experience. *Electronic Manufacturing Technology Symposium*, (32):332–334, 2007.
- [6] Klaus-Dieter Lang Otmar Deubzer, Nils F. Nissen. Overview of rohs 2.0 status of exemptions. *Electronics Goes Green*, pages 1–6, 2012.
- [7] Edward D Weil Sergei V Levchik. Thermal decomposition , combustion and flam-retardancy of epoxy resins- a reviw of the recent literature. *Polymer International*, 53:1901–1929, 2004.
- [8] Alun Morgan. Developments in glass yarns and fabric constructions. *The PCB Magazine*, pages 78–88, March 2014.
- [9] Samjid H. Mannan Hiren R. Kotadia, Philip D. Howes. A review: On the development of low melting temperature pb-free solders. *Microelectronics Reliability*, February 2014.
- [10] Holger Scharf Marion Hoppe Matthias Michaelis Julia Wienold, Sebastian Recknagel. Elemental analysis of printed circuit boards considering the rohs regulations. *Waste Management*, 31:300–305, November 2011.

- [11] Choong-Un Kim Hongtao Ma Tae-Kyu Lee, Thomas R. Bieler. *Fundamentals of lead-free solder interconnect technology*. Springer, 2015.
- [12] Sheng-Tsai Wu Ming-Che Hsieh and Chao-Huang Chen. Fracture analysis of interface delamination in metal-insulator-metal capacitor device. *Electronic System-Integration Technology Conference (ESTC)*, pages 1–5, 2010.
- [13] Steffen Wiese Joseph Al Ahmar. Fracture mechanics analysis on cracks in multilayer ceramic capacitors. *IEEE*, pages 1–5, 2014.
- [14] Michael Pecht Mohammadreza Keimasi, Michael H. Azarian. Isothermal aging effects on flex cracking of multilayered ceramic capacitors with standard and flexible terminations. *Microelectronics Reliability*, 47(12):2215–2225, 2007.
- [15] Tong Yan Tee Xueren Zhang. Advanced warpage prediction methodology for matrix stacked die bga during assembly processes. *Electronic Components and Technology Conference*, 1:593–600, June 2004.
- [16] M. Cermák R. Polanský, P. Prosr. Determination of the thermal endurance of pcb fr4 epoxy laminates via thermal analyses. *Polymer Degradation and Stability*, 105:107–115, April 2014.
- [17] N. J. Poole F. Sarvar and P. A. Witting. Pcb glass-fibre laminates: Thermal conductivity measurements and their effect on simulation. *Journal of Electronics Materials*, 19(12):1345–1350, July 1990.
- [18] J.Suhling J.Blanche M.Strickland P.Lall, V.Narayan. Effect of reflow process on glass transition temperature of printed circuit board laminates. *13th IEEE ITherm Conference*, 978(1):262–268, 2012.
- [19] IPC-TM-650 Test methods manual. *2.4.25 Glass Transition Temperature and Cure Factor by DSC*. Association Connecting Electronics Industries, Northbrook, IL, c edition, December 1994.
- [20] Erik Bergum Ed. Kelley. Laminate material selection for rohs assembly, part 1. *Printed Circuit design and manufacture*, 2006.
- [21] Ganesh Subbarayan-Dan Rose Thanate B. Ratanawilai, Brian Hunter. A study on the variation of effective cte of printed circuit boards through a validated comparison between strain gages and moiré interferometry. *IEEE transactions on components an packaging technology*, 26(4):712–718, December 2003.

- [22] The Institute for Interconnecting and Packaging Electronic Circuits. *2.4.24.1 Time to Delamination (TMA Method)*. IPC, Northbrook, IL, December 1994.
- [23] David Jennings Balu Rudra, Michael Pecht. Assessing time to failure due to conductive filament formation in multilayer organic laminates. *IEEE, Transactions on Components, Packaging and Manufacturing Technology*, 17(3):269–276, August 1994.
- [24] Michael Pecht Bhanu Sood. Controlling moisture in printed circuit boards. *IPC Printed Circuit Expo*.
- [25] M. Pecht Lili Ma, Bhanu Sood. Effect of moisture on thermal properties of halogen-free and halogenated printed-circuit-board laminates. *IEEE Transactions on device and materials reliability*, 11(1):66–75, March 2011.
- [26] IPC-TM-650 Test methods manual. *2.4.22c Bow and Twist (Percentage)*. Association Connecting Electronics Industries, Northbrook, IL, June 1999.
- [27] Christopher Robertson. *Printed Circuit Board Designer's Reference:Basics*. Prentice Hall PTR, 2003.
- [28] K. Azar J.E. Graebner. Experimental determination of thermal conductivity of printed wiring boards. *IEEE SEMI-THERM Symposium*, pages 169–182, July 1996.
- [29] Cemal Basaran Yujun Wen. An analytical model for thermal stress analysis of multilayered microelectronic packaging. *Mechanics of Materials*, 36:369–385, June 2004.
- [30] Ji Wu Michael Pecht Haiyu Qi, Sanka Ganesan. Effects of printed circuit board materials on lead-free interconnect durability. *Polytronic 2005 - 5th International Conference on Polymers and Adhesives in Microelectronics and Photonics*, 2005.
- [31] Sylvia Ehrler. The compatibility of epoxy-based printed circuit boards with lead-free assembly. *Circuit World*, 31(4):3–13, 2005.
- [32] Ravikumar Sanapala. Characterization of fr-4 printed circuit board laminates before and after exposure to lead-free soldering conditions. Master's thesis, University of Maryland CALCE, 2008.

- [33] Huiping Wang Yi Liu Yingfeng Yu Jie Zhang, Tian Li. Monitoring extent of curing and thermal-mechanical property study of printed circuit board substrates. *Microelectronics Reliability*, 54:619–628, December 2013.
- [34] Yuan Cao Haifeng Fiang Wenliang Zhu Shuo Xiao, Yang Zhao. Computing method of thermal conductivity of heat dissipation vias in printed circuit board and its optimization. *Circuit World*, 41(1):14–19, January 2015.
- [35] Tsuyoshi Nomura Masanori Ishigaki Ercan M. Dede, Paul Schmalenberg. Design of anisotropic thermal conductivity in multilayer printed circuit boards. *IEEE transactions on components an packaging technology*, 5(12):1763–1774, December 2015.
- [36] Edward Ramotowski Michal Baszynski, Mariusz Wojcik Mikko Kohvakka Dariusz Ostaszewski, Tomasz Klej, and Anssi Kamari. Evaluation of new technologies and materials for printed circuit boards with improved heat dissipation properties. *Circuit World*, 42(1):32–36, 2016.
- [37] Christine Harrington Eva McDermott, Bob McGrath. Long-term thermal reliability of pcb materials. *The PCB Magazine*, 6(4):58–82, April 2016.
- [38] T. Martin C. Umeagukwu R. Fulton C.P. Yeh, K. Banerjee and Motorola. Experimental and analytical investigation of thermally induced warpage for printed wiring boards. *IEEE*, pages 382–387, May 1991.
- [39] Carmine A. Puzzo Boris Djurovic and Jan K. Spelt. Analysis of thermal warpage in a pcb with an array of pth connectors. *IEEE, Transactions on Components, Packaging and Manufacturing Technology*, 22(3):414–420, 1999.
- [40] I. Charles Ume Wei Tan. Application of lamination theory to study warpage across pwb and pwba during convective reflow process. *IEEE, Transactions on Components, Packaging and Manufacturing Technology*, 2(2):217–223, February 2012.
- [41] Takashi Koyonagawa Michinobu Inoue. Thermal simulation for predicting substrate temperature during reflow soldering process. *IEEE Electronic Components and Technology Conference*, pages 1021–1026, June 2005.
- [42] Walter Sutherland Yarom Polsky, Charles Ume. Application of thermoelastic lamination theory to predict warpage of a symmetric and simply supported printed wiring board during temperature cycling. *IEEE*, pages 345–352, 1998.

- [43] Carl R. Hanna I. Charles Ume Hai Ding, Reinhard E. Powell. Warpage measurement comparison using shadow moiré and projection moiré methods. *Electronic Components and Technology Conference IEEE*, 25(4):714–721, December 2002.
- [44] Y.H. Lin C.Y Huang M.Y. Tsai M.C. Liao, P.S. Huang and T. C. Huang. Warpage measurements of printed circuit board during reflow process using strain gauges. *IEEE International Microsystems, Packaging, Assembly and Circuits Technology conference*, pages 397–400, 2014.
- [45] Yung-Chang Yii-Tay Chiou Chi-Chang Hsieh Yii-Der Wu Chi-Hui Chien, Thaiping Chen. Stability of the warpage in a pbga a package subjected to hygro-thermal loading. 2006.
- [46] Do-Hyoung Kim-Dong-Ok Kwak-In-Sang Song-Junhong Park Sung-Jun Joo, Buhm Park and Hak-Sung Kim. Investigation of multilayer printed circuit board (pcb) film warpage using viscoelastic properties measured by a vibration test. *Journal of Micromechanics and Microengineering*, 25(3), February 2015.
- [47] Paul P Conway-David J Williams David C. Whalley, Adebayo O Ogunjimi. A process model of the infra-red reflow soldering of printed circuit board assemblies. *IEEE*, pages 122–125, September 1991.
- [48] Paul P. Farhad Sarvar. Effective transient process modelling of the reflow soldering of printed circuit assemblies. *IEEE*, pages 195–202, May 1996.
- [49] David C. Whalley. A simplified model of the reflow soldering process. *IEEE*, pages 840–847, 2002.
- [50] Koichi Miyazaki Weiming Zhou Motohiro Yamane, Nobuaki Orita. Development of new model reflow oven for lead-free soldering.
- [51] Kousuke Nakao Etsuko Iwasaki. Development of high-speed pb-free reflow ovens. *Surface Mounting Engineering Department., Electronic Components Div. Electronics and Automotive Systems*.
- [52] Gábor Harsányi Zsolt Illyefavi-Vitéz-András Szabó Balázs Illés, Olivér Krammer. 3d investigations of the internal convection coefficient and homogeneity in reflow ovens. *IEEE, 30th ISSE*, pages 320–325, May 2007.
- [53] Ryohei Yokoyama Yasutada Nakagawa. Optimum design of printed circuit board to reduce deformation in reflow process by a global optimization method. 2011.

- [54] Soonwan Chung and Jae B. Kwak. Realistic warpage evaluation of printed circuit board assembly during reflow process. *Emerald Insight*, 27(4):137–145, June 2015.
- [55] S. Mercier L. Bodin-D. Manteigas B. Stephan A. Salahouelhadj, M Martiny. Reliability of thermally stressed rigid-flex printed circuit board for high density interconnect applications. *Microelectronics Reliability*, 54:204–213, September 2013.
- [56] M. Tonjec P.F. Fuchs, G. Pinter. Determination of the orthotropic material properties of individual layers of printed circuit boards. *Microelectronics Reliability*, 2012.
- [57] Paolo Emilio Bagnoli Yabin Zhang. A modeling methodology for thermal analysis of the pcb structure. *Microelectronics Journal*, 14:1033–1052, June 2014.
- [58] Cheikh-Tidiane Dia-Minh-Nhat Nguyen Valentin Bissuel Eric Monier-Vinard, Najib Laraqi. Analytical modeling of multi-layered printed circuit board dedicated to electronic component thermal characterization. *Solid States Electronics*, 103:30–39, October 2014.
- [59] Sylvia Ehrler. Pcb base material qualifications: discrepancies between supplier recommendations, customer abstract expectations and reality. *Emerald Insight*, 29(2):67–74, 2013.
- [60] Joseph Fjekstad. New material and process solutions for the electronic interconnection industry. *iconnect007*, 6(2):12–22, February 2016.
- [61] Research Center for Automotive. Contribution of the automotive industry to the economies of all fifty states and the united states. *Alliance of Automobile Manufacturers*, 2015.
- [62] Tackmo Lee-Minyoung Park Soonwan Chung, Seunghee Oh. Thermo-mechanical analyses of printed board assembly during reflow process for warpage prediction. *15th International conference on Thermal, Mechanical and Multi-Physics Simulation and Experiments in Microelectronics and Microsystems*, 2014.
- [63] Zhen Ding Technologies. Iphone 6s series drive sales of flex pcbs. *iconnect007*, 5(8):81, June 2015.

- [64] Association Connecting Electronic Industries. World production in 2014 estimated at 60.2 b. *iconnect007*, September 2015.
- [65] IDTechEx. Printed and flexible electronic in automotive applications 2016-2026:enabling technology toolkits, suppliers and market forecasts. *reportlinked*, April 2016.
- [66] IPC-TM-650 Test methods manual. *2.4.24.6 Decomposition Temperature (Td) of Laminate Material Using TGA*. Association Connecting Electronics Industries, Bannockburn, IL, April 2006.
- [67] IPC-TM-650 Test methods manual. *2.6.2.1 Water Absorption, Metal Clad Plastic Laminates Water Absorption, Metal Clad Plastic Laminates*. Association Connecting Electronics Industries, Northbrook, IL, a edition, May 1985.
- [68] P. Prosr J. Susir R.Polansky, V. Mentlik. Influence of themal treatment on the glass transition temperature of thermosetting epoxy laminate. *Polymer Testing*, 28(4):428–436, March 2009.
- [69] Diganta Das Michael Pecht Ravikumar Sanapala, Bhanu Sood. Effect of lead-free soldering on key material properties of fr-4 printed circuit board laminates. *IPC APEX EXPO Conference Proceedings*.
- [70] Weihong Yang Panagiotis evangelopoulos, Efthymios Kantarelis. Investigation of the thermal decomposition of printed circuit boards (pcbs) via thermogravimetric analysis (tga) and analytical pyrolysis (py-gc/ms). *Journal of Analytical and Applied Pyrolysis*, 115:337–343, August 2015.
- [71] The Institute for Interconnecting and Packaging Electronic Circuits. *2.4.24 Glass Transition Temperature and Z-Axis Thermal Expansion by TMA*. IPC, Northbrook, IL, c edition, 12 94.
- [72] E. Baylakoglu, I; Hedin. *The ELFNET Book on Failure Mechanisms, Testing Methods, and Quality Issues of Lead-Free Solder Interconnects*. Springer, 2011.
- [73] IPC-TM-650. *IPC-2221B Generic Standard on Printed Circuit Design*. IPC, 300 Lakeside, Drive, Suite 309S, Bannockburn, Illinois, November 2012.